An Ice Nucleation Study of Airborne Viruses

Mattie Hibbs

Department of Atmospheric & Oceanic Sciences

McGill University

Montréal, Québec, Canada

October 11, 2024

A thesis presented for the degree of Masters of Atmospheric and Oceanic Sciences

Abstract

Ice nucleation processes in the Earth's atmosphere are critical for cloud formation, radiation, precipitation, and climate change. Although some of the best known ice nucleating particles are of biological origin (bioaerosols), very little is known about the ice nucleation potential of airborne viruses. We investigated the physicochemical properties and ice nucleation potential of selected viral aerosols, including their RNA and proteins, using advanced techniques such as scanning-transmission electron microscopy (S/TEM), small angle X-ray scattering (SAXS), particle analyzers, and a Peltier chamber. The experiments revealed that RNA particles obtained from MS2 bacteriophage had a mean freezing point of -13.9 ± 0.3 °C, comparable to the average ice nucleation temperature of global dust particles, which induce freezing at approximately -15 °C. RNA from MS2, Influenza, SARS-CoV-1 and SARS-CoV-2 demonstrated average ice nucleation temperatures of -13.9 ± 0.3 °C, -13.7 ± 0.3 °C, -13.7 ± 0.3 °C, and -15.9 ± 0.4 °C, respectively. SAXS analysis indicated a high local crystallinity value of 0.5 of MS2 RNA particles, hinting that high crystalline nature may contribute to their effectiveness as ice nuclei. Drop-freezing experiments show that viral RNA consistently

catalyzes ice nucleation. The addition of dust-containing particles, such as Fe_2O_3, CuO, and TiO_2, to MS2 bacteriophage droplets enhanced ice nucleation, as did UV radiation. We herein discuss the implications of this work on atmospheric ice nucleation and freezing processes.

Résumé

Les processus de nucléation de la glace dans l'atmosphère de la Terre sont essentiels pour la formation des nuages, le rayonnement, les précipitations et le changement climatique. Bien que certaines des particules nucléantes les mieux connues soient d'origine biologique (bioaérosols), on sait très peu de choses sur le potentiel de nucléation des virus en suspension dans l'air. Nous avons étudié les propriétés physicochimiques et le potentiel de nucléation de la glace d'aérosols viraux sélectionnés, y compris leur ARN et leurs protéines, en utilisant des techniques avancées telles que la microscopie électronique en transmission à balayage (METB), la diffusion des rayons X aux petits angles, des analyseurs de particules et une chambre Peltier. Les expériences ont révélé que les particules d'ARN obtenues à partir du bactériophage MS2 avaient un point de congélation moyen de -13,9 ± 0,3 °C, comparable à la température moyenne de nucléation de la glace des particules de poussière globale, qui induisent une congélation à environ -15 °C. L'ARN de MS2, de la grippe, du SARS-CoV-1 et du SARS-CoV-2 a montré des températures moyennes de nucléation de la glace de -13,9 ± 0,3 °C, -13,7 ± 0,3 °C, -13,7 ± 0,3 °C et -15,9 ± 0,4 °C, respectivement. L'analyse de la diffusion

des rayons X aux petits angles a indiqué une valeur de cristallinité locale élevée de $0,5$ pour les particules d'ARN MS2, suggérant que la nature cristalline élevée peut contribuer à leur efficacité en tant que noyaux de glace. Les expériences de congélation de gouttes montrent que l'ARN viral catalyse systématiquement la nucléation de la glace. L'ajout de particules contenant de la poussière, telles que Fe_2O_3, CuO et TiO_2, aux gouttelettes de bactériophage MS2 a favorisé la nucléation de la glace, tout comme le rayonnement UV. Nous discutons ci-inclus des implications de ce travail sur les processus de nucléation et de congélation de la glace dans l'atmosphère.

Acknowledgements

I would first like to extend my gratitude to my supervisor Dr. Parisa A. Ariya for her support throughout my time at McGill. Under her guidance, I gained independence and confidence as a researcher. She challenged me to seek creative solutions and always encouraged me to dig deeper into topics that I was naturally curious about. I am also grateful for her role in creating a diverse and kind group of labmates, who have been a constant source of joy and camaraderie for me over the last three years.

I would specifically like to acknowledge my colleague Dr. Devendra Pal for being an incredible mentor and friend. I have learned so much from Dev about how to approach and overcome obstacles - both in the lab and in life. He is an inspiration and a fantastic teacher; I hope to emulate his mentorship style in the future when I am in a position to support a younger or less-experienced colleague.

I would like to thank my friends who have shown me endless support and who have given me a sense of family when I am so far away from home. The conversations we have had and the laughter we have shared have been integral to my overall health and well-being, and I

could not be luckier to have them in my life.

Lastly, I am deeply grateful for family; for my grandparents Jim and Mary who have played such an important role in my academic success; and for my parents' love and encouragement, not just in school but in all endeavors. They truly are my biggest fans.

Contribution of Authors

Mattie Hibbs is the primary author of this thesis. The introduction and literature review were written entirely by Mattie Hibbs. Editing and feedback were provided by the author's supervisor Dr. Parisa A. Ariya and a colleague, Dr. Devendra Pal.

The manuscript portion of this thesis has several authors: Mattie Hibbs, Devendra Pal, Gorjana Barudzija, and Parisa A. Ariya. The ice nucleation experiments were conducted by Mattie Hibbs and Gorjana Baruzija. Electron microscopy imaging was done by Dr. Vali. SAXS experiments were conducted by Dr. Hatem Titi at McGill University. Devendra Pal and Parisa Ariya provided guidance on experimental setup and methodology. Devendra Pal provided guidance on SAXS analysis, which was carried out by Mattie Hibbs. Figures and tables were created by Mattie Hibbs unless otherwise stated.

The manuscript has been submitted to the Royal Society of Canada journal *Environmental Processes and Impacts*, and has been accepted with revisions.

Contents

List of Figures

List of Tables

Chapter 1

Introduction

Ice nucleation, or droplet freezing, is a critical microphysical process in Earth's atmosphere (Kanji et al., 2017). When a suspended water droplet undergoes ice nucleation, the phase change also induces changes in the droplet's thermodynamic and optical properties (Chen et al., 2024; Irvine and Pollack, 1968); because clouds are mostly composed of water droplets and ice crystals, the transition between these phases (ice nucleation) plays an important role in determining a cloud's larger-scale thermodynamic, optical, and radiative properties (Burrows et al., 2022). Such properties are major sources of uncertainty in climate models, which currently use vast oversimplifications to characterize cloud composition and behavior (Matus and L'Ecuyer, 2017; Zelinka et al., 2017). Understanding microphysical atmospheric processes such as ice nucleation is essential for improving cloud parameterization in climate models.

One way to improve our understanding of atmospheric ice nucleation is to identify and examine airborne particles which may facilitate the phase transition; these are called Ice Nucleating Particles (INPs). It is well-known that some of the most efficient INPs are aerosols of biological origin, or bioerosols (Murray et al., 2012). Bioaerosols are ubiquitous in the atmosphere and generally fall into one of four categories: bacteria, pollen, fungi, or viruses (Kim et al., 2018). While numerous studies have been conducted on the ice nucleation potential of bacteria, pollen, and fungi, there is only one study to our knowledge which examines the ice nucleation ability of viruses (Adams et al., 2021).

This thesis is an investigation of the ice nucleation potential of airborne viruses and the physicochemical properties which may drive their ability to induce freezing. Subsequent sections of this introduction will provide an overview of the physical process of ice nucleation and review the current state of knowledge of ice nucleating particles.

1.1 Thermodynamics of Ice Nucleation

In order for water to freeze, it must overcome the free energy barrier, which demands that a certain amount of energy is added to the system for a reaction to occur (Schaller, 2019). Equation 1.1 gives the change in Gibbs free energy, ΔG, associated with the phase transition from a liquid water droplet to ice – i.e., the free energy barrier associated with ice nucleation.

$$\Delta \mathrm{G_{i,l}} = -\frac{4\pi r^3 \mathrm{R_v T}}{3\alpha_\mathrm{i}} \ln\left(\frac{e_\mathrm{sl}}{e_\mathrm{si}}\right) + 4\pi r^2 \sigma_\mathrm{i,w} \tag{1.1}$$

where r is the droplet radius, e_{sl} and e_{si} are the saturation vapor pressures with respect to liquid (l) and ice (i), and $\sigma_{i,w}$ is the surface tension at the interface of ice and water (Tan, 2022).

Although the theoretical freezing point of water is 0 °C, pure (uncontaminated) droplets freely suspended in the atmosphere can exist in a supercooled liquid state until around -40 °C, when they will eventually experience spontaneous freezing (Rogers and Yau, 1989). This type of pure-droplet freezing is called homogeneous ice nucleation. However, because most water droplets are contaminated, homogeneous nucleation is not often observed in ambient air. Rather, most water freezing events are heterogeneous - that is, occurring in the presence of other particles (INPs) or contaminants which can induce ice formation within a droplet at warmer temperatures.

1.2 Modes of Heterogeneous Freezing

There are several different modes of heterogeneous freezing: heterogeneous deposition, condensation and then freezing, contact freezing, and immersion freezing (Chou, 2011; Rogers and Yau, 1989). These modes are depicted in Figure 1.1.

In brief, heterogeneous deposition freezing occurs when ice forms directly on the nuclei from the gaseous (vapour) state and in the absence of supercooled liquid water. Condensation freezing first requires condensation of water vapour to liquid water on a particle, forming a droplet around the particle, and then freezing occurs from there. Contact freezing is

when a droplet freezes on contact with an INP. Lastly, immersion freezing occurs when the INP is already located inside of the water droplet in its liquid state, and then freezing is initiated. This is the most common ice nucleation mode in the atmosphere (Tobo, 2016) and is most relevant for mixed-phase clouds which form between -38 and 0 °C and are often glaciated to some degree by -20 °C due to heterogeneous ice nucleation (Whale, 2018). Unless otherwise stated, subsequent discussion of ice nucleation processes will be in specific reference to immersion mode freezing as it is the most atmospherically relevant freezing mode.

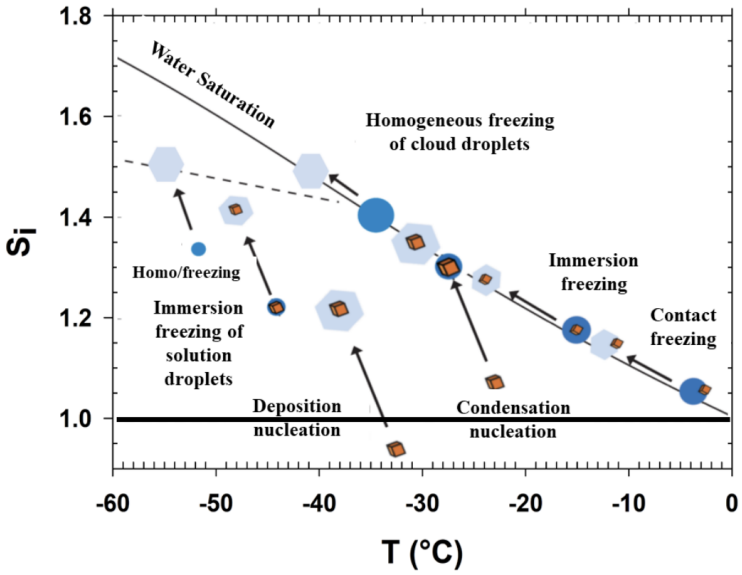

Figure 1.1: Schematic depicting the modes of freezing in the atmosphere as a function of temperature (T) and Supersaturation(S_i). Figure taken with permission from Pal (2023) who adapted the figure from Hoose and Möhler (2012).

1.3 Ice Nucleating Particles

1.3.1 Efficiency Requirements

There is no standard freezing temperature which deems an ice nucleating particle 'efficient.' In general, an INP which induces ice nucleation at a temperature closer to 0° C is more efficient than one which induces nucleation at lower temperatures (Ganguly et al., 2018b; Laaksonen and Malila, 2022). An INP's efficiency is determined by a multitude of microphysical and physicochemical properties (Pruppacher and Klett, 1997), which can make it challenging to determine the exact source of a particle's ice nucleation ability (INA). However, some of the major factors influencing a particle's INA are generally understood. Pruppacher and Klett (1997) posit five main requirements of a good ice nucleating particle, depicted in Figure 1.2. These requirements are with regard to an INP's solubility, size, chemical bond arrangements, crystallinity, and active sites.

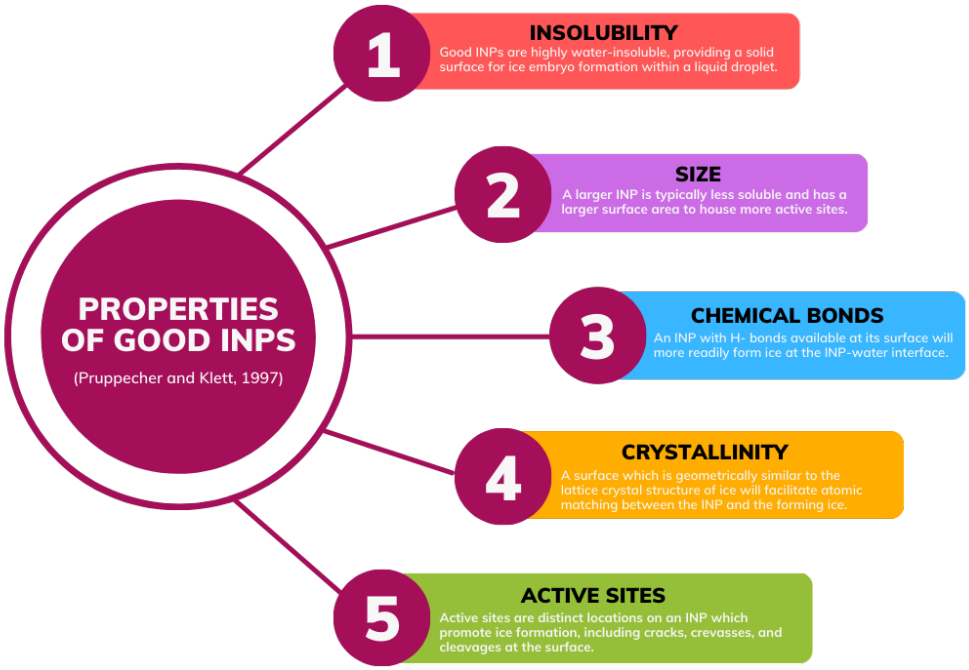

Figure 1.2: Properties of a good ice nucleating particle as outlined in Preppecher and Klett (1997).

1.3.2 Ice Nucleating Particles (INPs): Sources and Types

Ice nucleating particles exist in the atmosphere as suspended particulate matter which may originate from natural or anthropogenic sources (Hoose and Möhler, 2012). They can be a range of materials with a wide array of physiochemical properties and may be organic or inorganic (Kanji et al., 2017). It is important to note that a very small percentage of aerosols existing in the atmosphere can act as ice nuclei. Atmospheric concentrations of aerosols range from 10^2 – 10^4 cm^{-3}, while the concentration of ice nuclei is only 10^{-4} – 10^{-1}

cm^{-3}, several orders of magnitude smaller (Murray et al., 2012).

The most abundant ice nucleating particle in the atmosphere is dust, with an estimated global annual emission rate of 1000-3000 Tg/year (Murray et al., 2012). The term "dust" encompasses a variety of mineral types, including clay, feldspar, and quartz. Hoose et al. (2008) reported that mineral dust makes up about 77% of all active ice nuclei at temperatures warmer than -38 °C. Even though dust composition varies greatly depending on emission sources and geographic origin, there is evidence which suggests the specific mineral composition does not ultimately lead to large deviations in dust's ice nucleating ability (Kaufmann et al., 2016). On average, dust ice nuclei induce freezing around -15 °C (Murray et al., 2012; Hoose and Möhler, 2012).

Other categories of INPs include black and brown carbon, volcanic ash, sea spray aerosols, and bioaerosols. This project contributes to the existing body of literature on the latter – biological INPs. As such, the following section will review the main types of biological INPs (bacteria, fungi, pollen and viruses) and discuss what is already known about their ice nucleation abilities and mechanisms. A summary of studies involving other types of atmospheric INPs is given in Table 1.1.

Study	INP Type	Main Findings
DeMott (1990)	Black Carbon	IN active at T > -20 °C
Kanji et al. (2020)	Black Carbon	Completely inactive as an INP in immersion mode
Marcolli et al. (2021)	Black/brown Carbon (soot)	IN active by Pore Condensation Freezing (PCF) mechanism
Gao et al. (2022)	Black/brown Carbon (soot)	Larger INPs showed greater IN ability due to increaesed mesopore occurance and decreased mesopore width
Seifert et al. (2011)	Volcanic Ash	Cloud containing volcanic ash were glaciated by -15 °C; clouds without ash were not glaciated until <= -25 °C
Maters et al. (2019)	Volcanic Ash	Crystalline features in ash particles are critical to their INAs
Fahy et al. (2022)	Volcanic Ash	aqueous/chemical aging of ash immersed in supercooled water/aqueous sulfuric acid had a negative effect on its ice nucleating efficiency due to reduced crystallinity and active site occurrence
Bigg (1973) Schnell and Vali (1973)	Sea Spray Aerosols (SSA)	Ocean/marine environments contain 'copious' amounts of active INPs
Wilson et al. (2015)	Sea Spray Aerosols	Postulated that the ice nucleation ability of sea spray aerosols comes from resides in the organic content of the SSA, particularly phytoplankton organisms
Wagner et al. (2021)	Sea Spray Aerosols	Crystalline inorganic salts contributed to INA of SSAs

Table 1.1: Summary of findings from selected studies about the ice nucleation abilities of Black Carbon, Volcanic Ash, and Sea Spray Aerosols

1.3.3 Biological INPs

Bacteria

There are many types of bacteria that exhibit highly efficient ice nucleating ability. One of the most notable is the plant pathogenic bacteria *Pseudomonas syringae*, which induces

freezing between -2 and -7 °C (Huang et al., 2021). Other species of ice-nuclei active bacteria have been identified in the *Pseudomonadaceae*, *Enterobacteriaceae*, *Xanthomondaceae*, and *Lysinibacillus* families (Lukas et al., 2022).

It is currently understood that the freezing ability of certain ice-nucleating bacteria resides in proteins produced at the surface of the bacterial cell membrane. These proteins, called ice nucleating proteins, provide a template for surrounding water molecules to structure themselves into a crystalline, ice-like formation, thus lowering the kinetic barrier at the transition from liquid water to ice. The proteins are encoded in specific ice nucleation genes named inaZ, inaA, inaQ, etc (Lukas et al., 2022).

The physical structure of ice nucleation proteins can be broken down into three domains: the central repeating domain, an N-terminal domain, and a C-terminal domain (Lukas et al., 2022; Wolber, 1993). The central repeating domain (CRD) comprises about 81% of the ice nucleating protein structure and is likely where the active sites reside. The proteins form aggregates at the cell membrane surface; larger aggregations of these proteins correlate to freezing at warmer temperatures, and smaller aggregates correlate to freezing at colder temperatures, which is consistent with our knowledge of efficient ice nucleating particles (Lukas et al., 2022; Pruppacher and Klett, 1997). The physical process of protein aggregation is driven by both bacterial membrane conditions and environmental conditions, such as pH and electrostatic interactions (Lukas et al., 2020; Lukas et al., 2022). However, it is still not completely understood how to quantify the amount of ice nucleating proteins within the

aggregates or what specific interfacial interactions promote ice nucleation at the active sites. The exact biological structure of these proteins is still an active area of research.

Pollen

Pollen fragments have been shown to be effective ice nuclei in all heterogeneous modes of ice nucleation (Pummer et al., 2012). Many pollen particles in the atmosphere are too large to act as ice nuclei at high altitudes, because their size limits their vertical lofting; however, they often fragment or break into smaller pieces called sub-pollen particles (SPPs), which do have the ability to reach higher altitudes and act as ice nuclei at cloud-relevant heights (Gute et al., 2020). Gute et al. (2020) studied the ice nucleation ability of several varieties of SPPs in the immersion mode. They found that SPPs originating from gray alder trees exhibited a median freezing temperature of -6.5 °C, showing very high efficiency. Further work by Gute and Abbatt (2020) explored how the ice nucleation abilities of SPPs were altered as they were exposed to certain atmospheric factors, such as UV radiation, acidic water, and oxidation processes. It was found that the UV exposure most significantly affected the ice nucleating abilities by reducing the efficiency of the active sites, but that all exposure types had a negative effect on the ice nucleating ability. Thus, it was concluded that the ice nucleation abilities of SPPs may be reduced as they experience atmospheric aging.

While it is known that SPPs can be efficient ice nuclei, the microphysical mechanisms of the process is still an active area of research. Earlier work suggested that SPPs' ice

nucleation abilities could be attributed to their "rich surface topology" (Pummer et al., 2012). However, it was evident that this was not the full explanation, as pollens with similar topographic characteristics could exhibit very different freezing behavior. A more recent hypothesis is that the ice nucleation ability of pollen particles resides in macromolecules which are produced at the surface of the particles.

This so-called "macromolecule hypothesis" came about when Pummer et al. (2012) found that water which interacted with pollen had the same ice nucleating ability as the pollen itself; further examination revealed that pollen-produced macromolecules were suspended in the water and were likely responsible for the water taking on the same freezing ability as the pollen.

Dreischmeier et al. (2017) later examined the structure of the macromolecules released by birch pollen in water, and found that they were comprised of polysaccharides with carboxylate groups. Interestingly, the authors also found that the macromolecules exhibited anti-freeze properties, including ice recrystallization and ice shaping inhibition. The authors hypoothesized that the ice nucleation macromolecules could be aggregates of the smaller anti-freeze proteins naturally produced by the pollen for protection against night frost.

Fungi

Fusarium is a genus of fungi that exhibits notably high ice nucleation activity, with many of the species in this genus inducing ice nucleation above -7 °C (Pouleur et al., 1992). The genus was first identified as an active INP in a comprehensive 1992 study which looked at twenty different fungal genera and identified two *Fusarium* species which nucleated ice at temperatures warmer than -7 °C. It is now considered the most comprehensively studied ice nucleating fungus (Pouleur et al., 1992).

Like SPPs, the ice nucleation ability of *Fusarium* is thought to be driven by macromolecule production. Kunert et al. (2019) tested 100 different strains from 65 *Fusarium* species and found that roughly 16% of the strains induced freezing at temperatures warmer than -12 °C, and identified four new *Fusarium* species as active ice nucleating fungi. They also exposed these strains to different physical and chemical atmospheric factors such as ozone, nitrogen dioxide, and heat treatments. Notably, the heat treatments significantly decreased ice nucleation abilities, bolstering the hypothesis of macromolecule/proteinaceous-driven nucleation, as a protein will typically lose its shape, or denature, with heat treatment (Davis and Williams, 2008).

Other fungi have been investigated for ice nucleating abilities, although none as extensively as those in the *Fusarium* genus. A study by Iannone et al. (2011) examined the ice nucleation ability of fungal spores in the *Cladosporium* genus, which is one of the most abundant fungal spores in the atmosphere. However, these spores exhibited relatively poor

nucleation abilities, with mean freezing temperatures around -35 °C. The authors suggested that the reason for such poor efficiency is that *Cladosporium* fungi are coated with hydrophobic proteins; it is well-known that hydrophobic surfaces do not generally serve as efficient ice nuclei (Pruppacher and Klett, 1997).

Viruses

A 2017 study investigated the INP composition of rainwater samples taken from northern China (Du et al., 2017); they found evidence of submicron ice nucleating particles that could not be identified as any known ice-nucleating bacteria or fungi. The authors suggested that there may be a "missing source" of highly efficient submicron INPs, and that viruses are one possibility.

Viruses are the least studied of the biological INPs, but they are potentially good candidates for INP investigations. Their small size and light weight allow them to have longer atmospheric residence times and experience long-range transport (Chen et al., 2021). They are also ubiquitous on the Earth; there are an estimated 10^{31} viral entities present in the biosphere (Breitbart and Rohwer, 2005; Moelling and Broecker, 2019). Viruses may be transferred to the atmosphere by natural weather phenomena (wind, rain) or by emission from a host. Once in ambient air, viruses may interact with other existing aerosols and undergo atmospheric processes or participate in microphysical processes, including ice nucleation.

While several viruses can indeed nucleate ice at temperatures above -25 °C, the specific microphysical mechanisms of ice nucleation is not well understood. Adams et al. (2021) experimented with eight common viral structures to determine if their architectures were responsible for their ice nucleating abilities. The study found that the viruses did have ice nucleating abilities but it did not find any significant relationship between their various architectures/structures and their respective abilities (Adams et al., 2021). It is important to note that the study only examined a small amount of virus types which infect plants, and did not examine human or animal viruses. Further, it has been shown that there are other viruses which exhibit ice nucleating ability, although none have been extensively investigated (Cascajo-Castresana et al., 2020).

1.3.4 Outstanding Questions

There are certainly questions remaining about the ice nucleation efficiencies and mechanisms of the various biological ice nucleating particles, but none moreso than viruses, with just one single paper examining their ice nucleation potential (Adams et al., 2021). Unlike the other biological INPs outlined in this introduction, it is almost completely unknown if viruses may serve as efficient ice nuclei, and there has been no work which has examined the mechanisms of viral particle freezing. The manuscript within the next chapters of this thesis explores the following questions:

1. What is the ice nucleation efficiency of airborne/respiratory viruses?

2. Can viral remnants, proteins, or fragments serve as ice nucleating particles?

3. What surface properties may play a role in the freezing process of viral droplets?

1.3.5 Thesis Structure

The remainder of this thesis contains an original manuscript which addresses the questions above. The subsequent sections are as follows:

Chapter 2 is the manuscript introduction, discussing the motivation for examining the ice nucleation potential of airborne viruses.

Chapter 3 details the methodology in this study, including the experimental set-ups, materials and supplies, and analytical methods.

Chapter 4 contains the results and a discussion of the findings.

Chapter 5 gives concluding remarks and discusses potential future work on this topic.

Chapter 2

Motivation and Background

The Intergovernmental Panel on Climate Change (IPCC) has identified airborne particles, or aerosols, as a priority research area for air quality and climate change (Boucher and Randall, 2013; Penner et al., 2018). Air pollution and, notably, small aerosols cause around 7 million premature deaths every year globally, making them an important topic in health science research (Lelieveld et al., 2020). Furthermore, aerosols are critical to several atmospheric processes, including cloud formation, precipitation, the radiation budget, and global climate change. Understanding physicochemical properties such as size, shape, abundance, and surface topography of aerosols, particularly bioaerosols, is crucial for assessing their role in aerosol-cloud interactions (Grassian, 2008; Ariya et al., 2009; Rangel-Alvarado et al., 2021).

Bioaerosols are aerosols of biological origin or those containing biological parts or derivatives, including bacteria and viruses (Kim et al., 2018). Viruses exist ubiquitously in

the natural environment, including in soil, water, and air. Their numbers are greater than any other biological entity with an estimated 10 nonillion (10^{31}) individual viruses on Earth (Moelling and Broecker, 2019; Geographic, n.d.). Airborne viruses can interact with other aerosols in the atmosphere and may experience long-range transportation and may undergo physicochemical transformations (Sun and Ariya, 2006). These physicochemical changes are influenced by the aerosols' microphysical characteristics and by atmospheric conditions such as humidity, temperature, and radiation (Yang and Marr, 2012; Baboomian et al., 2020; Walhout et al., 2019; Koohbor et al., 2023). Although a comprehensive understanding of the physicochemical properties of bioaerosols is necessary for assessing their impact on atmospheric chemistry processes and epidemiological processes (Morawska et al., 2022; Pal et al., 2023), their role as ice and cloud condensation nuclei remain an active research area.

In recent decades, various emerging contaminants have been identified as effective ice nuclei, specifically contaminants originating from nano/microplastics (Ganguly and Ariya, 2019), metal-organic complexes (Ganguly et al., 2018a), and pharmaceutical materials (Kaur et al., 2022). While dust particles are known to be the most abundant type of ice nucleating particles in the atmosphere, certain bioaerosols are among the most efficient (Murray et al., 2012; Iwata et al., 2019). For example, *Pseudomonas syringae* bacteria have evolved to induce ice nucleation within a temperature range of approximately -2 to -7 ℃ (Lukas et al., 2022). In comparison, dust particles exhibit ice nucleation abilities around -15 ℃ (Murray

et al., 2012; Hoose and Möhler, 2012). The ice nucleation mechanisms of various bioaerosols including pollen (Hartmann et al., 2022), fungi (Pouleur et al., 1992), and bacteria (Lukas et al., 2022) have been extensively studied, but very little is known about the ice nucleation ability of airborne viruses (Adams et al., 2021).

In this study, we investigated the ice nucleation abilities of airborne viruses and their RNA, along with the impact of mixing the viruses with dust particles. We conducted microphysical experiments focusing on MS2 Bacteriophage (also termed Bacteriophage MS2 or MS2), a single-stranded RNA virus infecting *Escherichia coli*. MS2 is a commonly found virus and it, along with other bacteriophages, serves as a good surrogate for studying airborne viruses (Turgeon et al., 2014). Additionally, we assessed the ice nucleation abilities of viruses such as SARS-CoV-1 RNA, SARS-CoV-2 RNA and proteins, RNA from human influenza, and heat-inactivated SARS-CoV-2 (COVID-19). Furthermore, we performed surface property analysis on the viruses to understand their potential role on ice nucleation mechanisms. The implication of our findings is discussed herein.

Chapter 3

Methodology

A common way to study the ice nucleating ability of ice nucleating particles (INPs) is drop freezing assay experiments, which have been shown by Vali (1971) to be an accurate method for calculating the active ice nuclei content of the solution from which the droplets were formed. Drop freezing experiments are characterized by the simultaneous cooling of equal-sized droplets until frozen, and the freezing point of each droplet is recorded. Based on the observed freezing temperatures, the differential nuclei concentration k(T) can be obtained (*Methods: Ice nucleation - analysis, Eqn. (3.1)*).

In this study, we conducted drop freezing assays of viral droplets using a laboratory-built ice nucleation apparatus (Mortazavi et al., 2008; Côté et al., 2008). In brief, solutions containing either viral particles or some mixture of viral particles with other common aerosols, were made by dilution using ultrapure Milli-Q water (18.2 $M\Omega \cdot cm$

Milli-Q Synergy UV system, Millipore Sigma, USA). MS2 viral solutions were prepared at varying concentrations of 100 X, 200 X and 330 X. To ensure an even distribution of particles, all solutions were vortexed. Each experiment comprised approximately 120 droplets of equal volume (10 μL) deposited onto a Vaseline-coated copper plate and replicated trice. Once each droplet was placed uniformly on the freezing plate, the plate was cooled at a constant rate of 0.9 degrees centigrade per minute, and the temperature at which the liquid droplet solidified was recorded. To verify that all freezing events were captured, we recorded a video for cross-verification.

We also investigated the impact of mixing with dust particles (nanosized Fe_2O_3, CuO, and TiO_2) and UV exposure on the ice nucleation ability of MS2. To examine how ice nucleation changes when viral droplets are clustered together, designated samples were briefly centrifuged for 2-5 minutes to promote particle agglomeration. To assess the impact of light on viral droplets, MS2 samples were exposed to UVA (315-400 nm) or UVB (280-315 nm) irradiation for 30 minutes.

3.1 Ice nucleation - analysis

The differential nuclei concentration k(T) (in nuclei * L^{-1}) describes the average number of ice nuclei in a temperature interval, n(T), per unit of volume, V, and can be expressed as:

$$k(T) = \frac{n(T)}{V} \tag{3.1}$$

Upon algebraic rearrangement and integration, the cumulative concentration of active ice nuclei, K(T) (in nuclei * L^{-1}) is obtained:

$$K(T) = \frac{\ln N_0 - \ln N(T)}{V} \tag{3.2}$$

where N_0 is the number of droplets in the initial population and N(T) is the number of unfrozen droplets at temperature T (Vali, 1971).

All data processing, statistical analysis methods, and plotting methods/software are discussed in *Methods: Statistical Analysis and Plots.*

3.2 Litesizer particles sizer

Litesizer particle sizer 500 (PSA, Anton Paar) was used to analyze the particle diameters distributions, diffusion coefficients, and transmittances of MS2 samples. The PSA instrument uses dynamic light scattering to obtain information about the physical properties of the samples. Three measurements were made for each sample at 25 °C with the default measurement angles of 15°, 90°, and 175°.

3.3 Electron microscopy imaging

Talos F200X scanning/transmission electron microscope (S/TEM) was used. Talos combines high resolution S/TEM and TEM imaging, with energy dispersive X-ray spectroscopy (EDS), which allows signal detection and elemental analysis of selected areas. The imaging was performed by the Facility for Electron Microscopy Research at McGill University. Bacteriophage MS2 was prepared for S/TEM imaging by staining with uranyl acetate and the Spirit 120 kV TEM was used for imaging. Another set of MS2 samples was prepared without uranyl acetate staining to determine the composition of the material on the grid and was imaged in the Talos F200X 200 kV TEM.

3.4 Heat inactivation of SARS-CoV-2 virus

In a biosafety 3 laboratory, a specific volume of SARS-CoV-2 was heat-inactivated at 92 °C for 1 hour with continuous shaking to ensure biosafety during subsequent handling in a biosafety level 1 laboratory setting. Figure A.1 shows the heat inactivation images of the SARS-CoV-2 sample, and figure A.2 shows the BLAST results of sequenced genome confirming the SARS-CoV-2 identity. Methods for heat inactivation of SARS-CoV-2 usually use temperatures of around 56 – 60 °C (Pastorino et al., 2020; Batéjat et al., 2020; Kampf et al., 2020) although those methods are typically used to only reduce the viral activity when the sample is needed for serological assays. A few studies have also examined the

remaining infectivity when SARS-CoV-2 samples are exposed to 80 °C for 1 hour , 92 °C for 15 minutes (Batéjat et al., 2020) and 95 °C for 3 minutes (Kampf et al., 2020). We performed heat inactivation at 92 °C for 20 minutes; viral activity was still observed and theore the exposure time was increased to one hour.

To confirm no remaining live virus, the inactivated virus was tested by inoculating host cells. The test sample was passaged twice; the first passage was incubated for 3 days, and the second passage was incubated for 7 days. Vero E6 confluent monolayers were infected with SARS-CoV-2 virus (MOI 0.05), heat-inactivated SARS-CoV-2, and monitored for cytopathic effect (CPE). On day 3, the supernatant was removed, spun down to remove any cell debris, and then transferred to a new lot of Vero E6 confluent monolayers and monitored for 7 days. Heat-Inactivated SARS-CoV-2 using this protocol did not cause infection as determined by the lack of CPE in the inoculated Vero E6 cells. RIM-1, lineage B.1.147 was used for heat-killed samples (formally called CP13.32) which was SARS-CoV-2 that was propagated from a McGill University Health Center (MUHC) patient sample from March/April 2020. The RIM-1 viral stocks were whole genome sequenced, and the GenBank accession number is MW599736. Images of inactivated viruses are given in Supplementary Information Figure A.1.

3.5 Small angle x-ray scattering (SAXS) analysis

The SAXSpoint 2.0 (Anton Paar, Austria) at McGill University was used to analyze physical properties of MS2 bacteriophage samples. The SAXS instrument employed a CuKα radiation source with a wavelength ($\lambda = 1.54\mathring{A}$) and an Eiger R 1M (Horizontal) detector. The source-to-detector distance was set at 576.33 mm for the experiments. 30 μL of sample volume was used during each experiment and placed in quartz capillary (1 mm, Anton Paar). During each measurement, a total of 3 frames were recorded with 20 minutes per frame of X-ray exposure. The obtained SAXS profiles were corrected as a function of the scattering vector ($q = (4\pi/\lambda)\sin\theta$, where 2θ is the scattering angle). Data analysis of the SAXS measurements was performed using SasView 5.0.4 software, an open-source code widely used for SAXS data analysis ("SasView User Documentation — SasView 5.0.6 documentation", n.d.). The Milli-Q water was used as background data; it has been subtracted from all the measured samples and the normalized dataset was used for subsequent analysis (SAXSpoint 2.0). The SASView software was also used for Guinier analysis to check the data quality. Correlation function analysis was performed to extract the surface properties, including the polydispersity, average core thickness, and local crystallinity of each sample. The user specified the q-ranges of analysis, and the software extracted these properties/parameters using a Guinier function to fit the designated low-q range values, and a Porod model for fitting the high-q range values (Bose et al., 2024).

Polydispersity is calculated in the software by dividing the standard deviation of the size

distribution by the mean size value. Local crystallinity is calculated by dividing the average hard block thickness (L_c) by the long period (L_p).

3.6 Statistical analysis and plots

Various statistical analyses were performed to investigate the ice nucleation efficiency of the different samples. The reported results include 1^{st} and 99^{th} percentiles, along with median and average values. Two-sample t-tests were performed in RStudio using the t.test function, in which it assumed that the two populations have different variances. Standard errors were calculated via the following equation appropriate for large sampling data, where σ corresponds to the standard deviation and N is the sample size.

$$SE = \frac{\sigma}{\sqrt{N}} \tag{3.3}$$

All graphs were made in in RStudio. Data is publicly available on the Borealis Data Repository (Hibbs, 2024).

3.7 Materials and Supplies

The metal oxides used were Fe_2O_3, CuO, and TiO_2; they were purchased from Sigma Aldrich in nanoparticle form. SARS-CoV-1 RNA and RNA from Bacteriophage MS2

(product code: 10165948001) were purchased from Sigma Aldrich. Bacteriophage MS2 (0810052) was manufactured by Zeptometrix Corporation and supplied by Cedarlane Laboratories. Influenza RNA (VR-95DQ) was manufactured by American Type Culture Collection and supplied by Cedarlane Laboratories. SARS-CoV-2 RNA (ssRNA, EURM019) was supplied by the Joint Research Centre (European Commission), and proteins were supplied by Life Technologies Inc. SARS-CoV-2 was propagated and then heat inactivated in a BSL3 laboratory at the Research Institute of the McGill University Health Centre (RI MUHC).

3.8 A note on terminology

In this paper, we use the terms *virus* and *viral particle*. *Virus* is the general term for what we are studying; SARS-CoV-1, SARS-CoV-2, Influenza, and MS2 bacteriophage are all viruses. A *viral particle* is a particle containing viral material.

Chapter 4

Results and Discussion

In this study, we conducted a comprehensive series of ice nucleation microphysics experiments involving various viral components, including the model virus MS2 Bacteriophage and its RNA, heat-inactivated SARS-CoV-2 (COVID-19), SARS-CoV-2 RNA, and SARS-CoV-1 RNA and proteins. Our goal was to investigate the ice nucleation abilities of these viral components and compare the results with proxy dust particles. Furthermore, we explored the influence of mixing with dust particles and the impact of UV radiation on the virus' respective ice nucleation abilities. A summary of the mean freezing ice nucleation temperatures of various samples is given in Figure 4.1.

4.1 Ice nucleation of bacteriophage MS2: Impact of UV light exposure

Figure 4.1 and Figure 4.2(a) show the mean freezing temperatures from drop-freezing experiments for MS2 Bacteriophage at different dilutions (100 X, 200 X, 330 X). The mean freezing temperatures for samples of MS2 Bacteriophage at 100 X, 200 X and 330 X dilutions were -16.5 ± 0.3, -18.8 ± 0.3 , and -18.2 ± 0.3 °C, respectively (Fig. 4.1, red box). We observed that the mean freezing temperatures decreased by about 2 °C with an increased dilution factor from 100 X to 200 X, and no significant change in subsequent dilutions. This may likely be due to decreased particle concentration affecting ice nucleation site availability, thus slowing down the catalytic process Raatikainen et al., 2022). Interestingly, MS2 RNA exhibited a mean freezing temperature of -13.9 ± 0.3 °C, indicating RNA may have high efficiency as an ice nucleating particle (Fig. 4.1).

To investigate the impact of irradiation on the ice nucleation ability of airborne viruses, we exposed 100 X diluted MS2 samples to UVA (315-400 nm) and UVB (280-315 nm). The mean freezing values of UVA- and UVB-exposed MS2 samples were -13.4 ± 0.4 and -12.6 ± 0.3 °C, respectively, and the cumulative nucleus concentration of photolyzed MS2 and centrifuged photolyzed MS2 samples are shown in Figure 4.2(b).

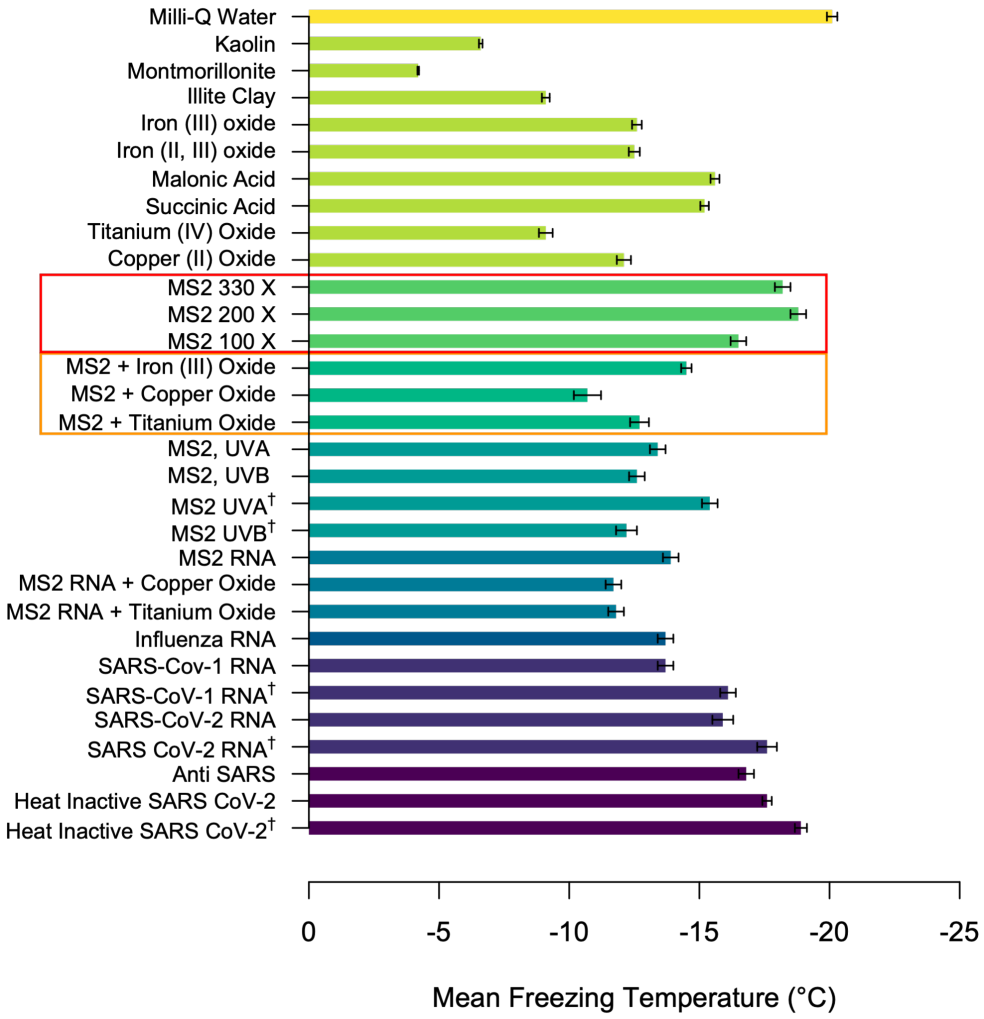

Figure 4.1: Mean freezing temperatures from drop freezing experiments of various samples; †Centrifuged.

A t-test (p = 0.108) confirmed no significant difference in ice nucleation results between UVA- versus UVB- exposed MS2-100 X samples, but a significant (p « .00001) difference was indeed observed between untreated MS2-100 X mean freezing temperatures and both UV-treated samples (Fig 4.1, and Fig. 4.2(b)). UVA exposure elevated the freezing

temperature by -3.1 °C and UVB elevated it by -3.9 °C. This indicates that UV radiation may increase the ice nucleation potential.

4.2 Mixing MS2 with Dust-like particles: Impacts on ice nucleation

We examined the impact of mixing MS2 with common metal oxides found in dust particles such as TiO_2, Fe_2O_3 and CuO nanoparticles. We exposed viral MS2-100 X dilution samples at 0.1% solutions of TiO_2, Fe_2O_3 and CuO. The mean freezing temperatures are given in Figure 4.1 (orange box), and Figure 4.2(c) shows the cumulative nucleus concentration of MS2 compared with the mixtures of MS2 with dust particles. The mean freezing temperatures of MS2-100X diluted sample alone was -16.5 ± 0.3 °C; when MS2 was mixed with TiO_2, Fe_2O_3 and CuO, the freezing temperatures increased to -12.7 ± 0.2, -14.4 ± 0.2 and -10.7 ± 0.3 °C, respectively. These findings suggest that the presence of dust particles can enhance the ice nucleation ability of viral particles, likely due to increased surface area and effective ice nucleation sites provided by the dust particles (Pruppacher and Klett, 1997). A statistically significant difference ($p < 0.05$) was found between the mean freezing temperatures of the MS2-100 X sample, and the MS2-100 X mixture samples. Figures A.3 and A.4 in Supplementary Information show the cumulative nucleus concentrations of a selection of airborne particles (A.3) as well as TiO_2, Fe_2O_3 and CuO (A.4).

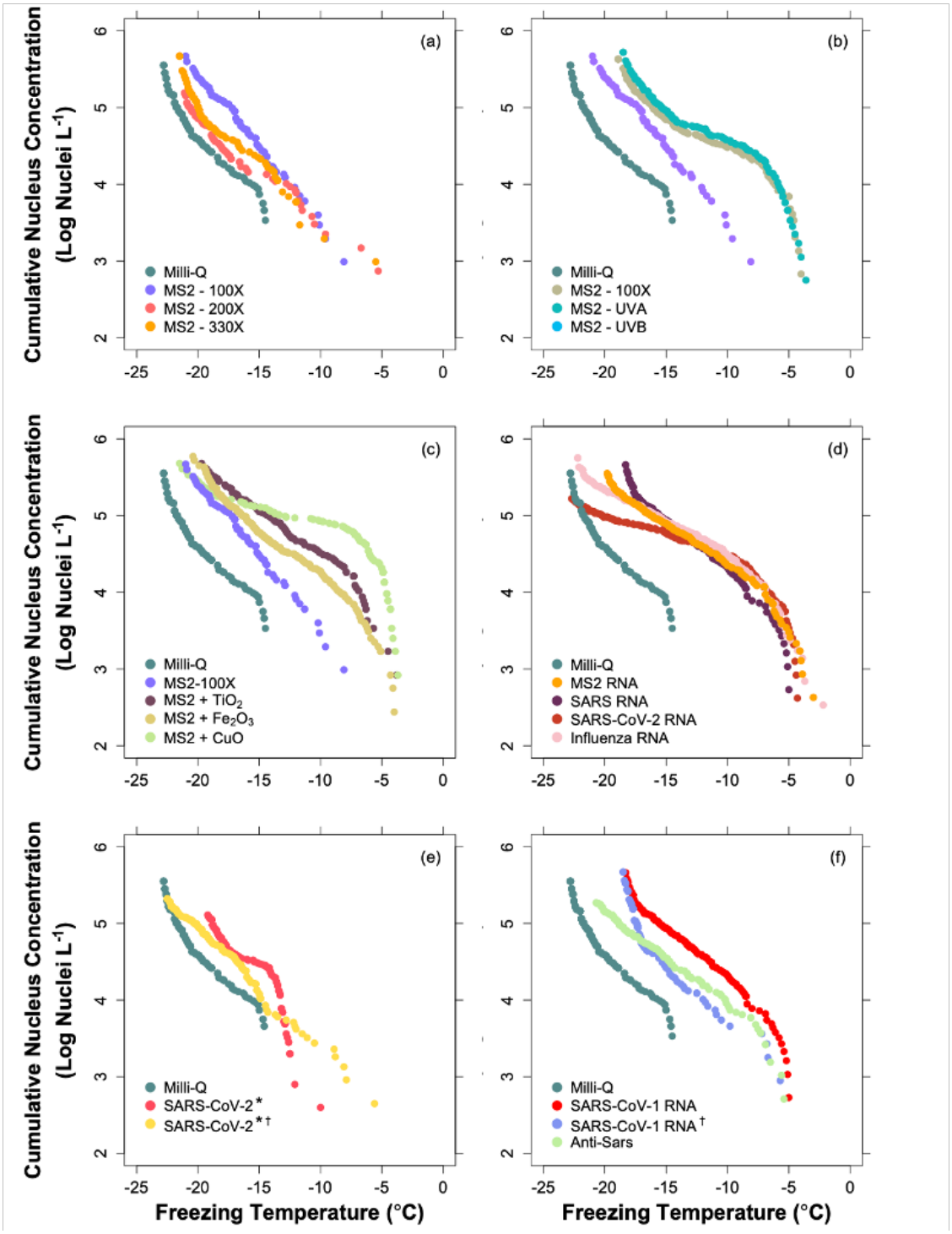

Figure 4.2: Cumulative nucleus spectra obtained from drop-freezing experiments of (a-c) different MS2 solutions, (d) viral RNA, (e) treatments of SARS-CoV-2, and (f) treatments of SARS-CoV-1 RNA. †Centrifuged; *Heat-Inactivated.

4.3 Ice nucleation of SARS-CoV-2, RNA and related samples

Heat inactive SARS-CoV-2 had a mean freezing temperature of -17.6 ± 0.4 °C, which decreased further upon centrifugation to -18.9 ± 0.2 °C. It is essential to consider that the heat inactivation process may lead to the presence of fragmented RNA and protein shells in the sample, potentially affecting its ice nucleation behavior. Ice nucleation of these coronaviruses-related samples show that even when a viral droplet contains an inactive virion, it still has the potential to be a good INP.

Furthermore, we investigated the ice nucleation efficiency of several RNA samples, considering many airborne viruses are RNA Viruses (Hodinka, 2016). The ice nucleation efficiencies of RNA from MS2, SARS-CoV-1, SARS-CoV-2, and Influenza was investigated. Viral RNA, enclosed within the capsid, can degrade under certain atmospheric conditions, such as high relative humidity or reactive oxygen species (ROS), potentially leaving RNA fragments in the atmosphere (Colas de la Noue et al., 2014). Viral RNA exhibits high mutation rates and morphological diversity (Durmuş and Ülgen, 2017), making it suitable for studying ice nucleation processes that depend on particle structure and morphology (Pruppacher and Klett, 1997).

The ice nucleation efficiencies and cumulative nucleus concentrations of RNA from MS2, SARS-CoV-1, SARS-CoV-2, are shown in Figure 2d. The mean freezing

temperatures of RNA from MS2, SARS-CoV-1, and Influenza were -13.9 ± 0.3, -13.7 ± 0.3, and -13.7 ± 0.3 °C, respectively (Fig 4.1), revealing that RNA freezes at warmer temperature than some ice-nucleating dust particles (Fig 1). Figures 4.2(e) and 4.2(f) show the cumulative nucleus concentrations of SARS-CoV-1 RNA and SARS-CoV-2 RNA as well as the centrifuged samples. Centrifugation in these experiments did not significantly affect the ice nucleation abilities of either RNA type.

In this study, our primary focus has been on using deactivated viruses to ensure health and safety during the experiments in our microphysics labs, acknowledging that the ice nucleation behavior is expected to be altered. Furthermore, some S/TEM and BET facilities cannot host even deactivated viruses. Using different preparation methods, all RNA tested displayed ice nucleation efficiency, demonstrating that the various methods of RNA isolation are not likely the cause of ice nucleation, but that the RNA itself is. It is important to clarify that when we er to RNA as an ice-nucleating particle, we are considering the entire structure of the RNA, including the capsomeres. However, we do not make specific claims about whether the ice nucleation ability resides strictly in the genetic material or within the capsid's system, as that is beyond the scope of this paper. Yet, we recommend future research in this domain.

4.4 Surface properties and ice nucleation efficiency

Small-angle X-ray scattering (SAXS) measurements provide crucial insight into the nanoscale density differences in both solid and aqueous samples (Li et al., 2016; Boldon et al., 2015). These density differences determine the particle size distribution, shape, dispersity (monodispersed and polydispersity), pore size, and local crystallinity, which are essential for assessing ice nucleation capabilities (Pal et al., 2023; Wagner et al., 2016). The scattering data obtained from SAXS measurement contains information on the size, shape, orientation, squared contrast, weighted concentration, and volume of the particles. For this study, we used SasView5.2 software for correlation function analysis to estimate the changes in phase or orientation change in particles, affecting local crystallinity (phase) of the materials (SasView, n.d.). Table 4.1 presents the local crystallinity and polydispersity of MS2 samples. Polydispersity measures the width of the size distribution of correlation function decay rates and not the particle size distribution("SasView User Documentation — SasView 5.0.6 documentation", n.d.). The change in phase (local crystallinity) and polydispersity of material significantly impacts the ice nucleation capability of materials (Kaur et al., 2022; Bose et al., 2024).

In this study, we analyzed three MS2 samples (100 X, 200 X and 330 X) to understand their physical properties and their role in ice nucleation mechanism. The MS2-100 X sample exhibited higher local crystallinity and similar polydispersity compared to MS2-200 X and MS2-330 X, shown in Table 4.1. The combination of high polydispersity and local

crystallinity likely makes the MS2-100 X sample more efficient at ice nucleation. A higher degree of crystallinity suggests a greater potential for the sample to organize neighboring water molecules into ice-like crystal formations, enhancing its ice nucleation capability (Kaur et al., 2022; Pruppacher and Klett, 1997). Conversely, MS2-330 X, with slightly higher polydispersity but significantly lower local crystallinity, and MS2-200 X, with similar polydispersity but lower crystallinity than MS2-100 X, induced ice nucleation at cooler temperatures (Figure 4.1). Theore, a higher degree of crystallinity in the samples suggests a stronger ice nucleation capability.

The overall effectiveness of ice nucleation depends on the combined effect of both local crystallinity and polydispersity. Materials with high crystallinity and higher polydispersity tend to have polymorph surfaces, which lowers the free energy, enhances local structuring upon cooling, and promotes crystallization in a supercooled state, causing droplets to freeze at warmer temperatures (Bose et al., 2024). Density, poly-surfaces, and polydispersity are control parameters that induce crystallization and favor structures acting as precursors for the ice nucleation process.

The SAXS intensity counts of the three different MS2 dilution samples are shown in Figure 4.3. The observations suggest the MS2-100 X had the highest scattering intensity, while the more diluted samples had very similar scattering patterns to each other. These results are likely due to the increased concentration of viral particles in the 100 X solution. Further dilutions have reduced viral particles concentrations, and thus they more closely

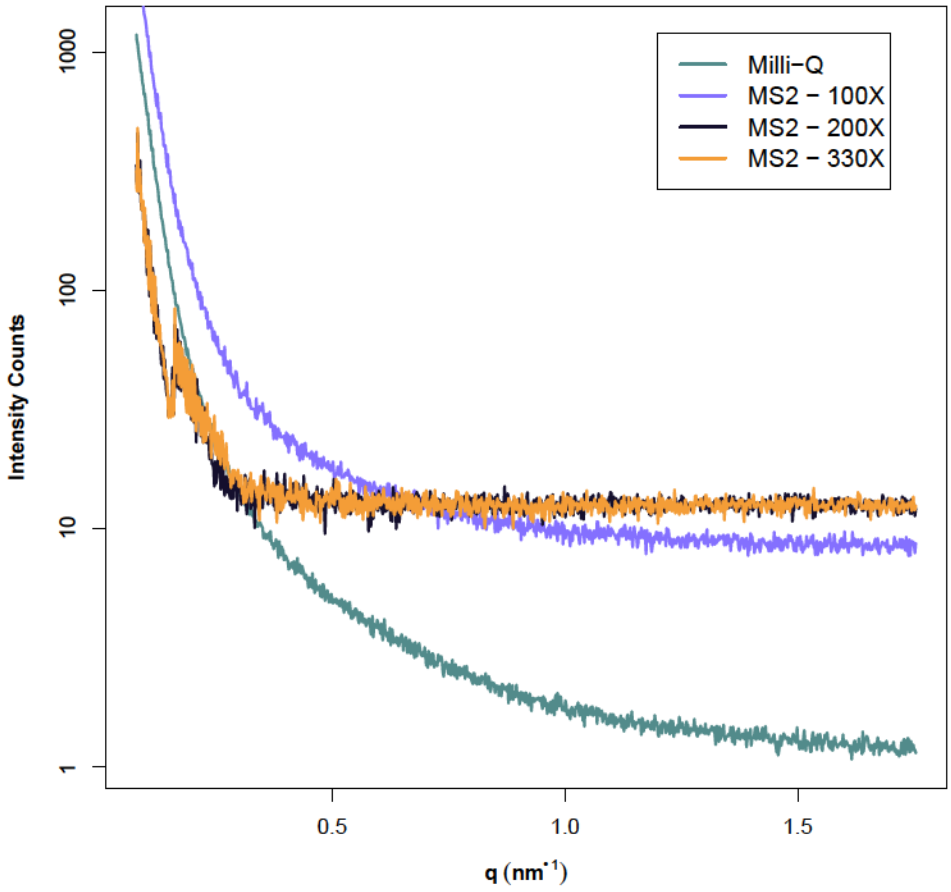

Figure 4.3: Intensity counts of MS2 at 100 X, 200 X and 330 X dilutions obtained from SAXS analysis plotted on a log scale.

resemble the Milli-Q blank.

Furthermore, Litesizer particle sizer data includes the diffusion coefficients and transmittance, shedding light on surface physiochemistry. These coefficients provide valuable information about the movement of particles, dispersion, and stability in the

solution and the extent to which light is transmitted through the sample. These are not necessarily predictors of excellent or poor ice nuclei but serve as supplemental data to show the internal structure of a solution of viral particles in water. We saw no significant difference between water and viral solutions' transmittance and diffusion properties but a considerable difference between these samples and the mixtures with dust particles.

SAXS Correlation Function Analysis Parameter			
Sample	**Polydispersity**	**Avg. Core Thickness (Å)**	**Local Crystallinity**
MS2 100 X	2.44	9.2	0.512
MS2 200 X	2.4	7.0	0.388
MS2 330 X	2.79	7.2	0.282

Litesizer Particle Sizer Physical Properties				
	Diffusion Coefficient		**Transmittance**	
Sample	**Measurement 1**	**Measurement 2**	**Measurement 1**	**Measurement 2**
Milli-Q	0.737	0.615	87.5%	87.6%
MS2 100 X	1.60	1.83	87.2%	87.2%
MS2 200 X	1.82	1.48	87.9%	87.9%
MS2 330 X	1.59	1.59	87.7%	87.7%
MS2 + Fe_2O_3	4.68	4.76	10.6%	10.9%

Table 4.1: (Top) Physical properties of MS2 samples extracted from SAXS data with SasView software. Properties include polydispersity, average core thickness, and local crystallinity. **(Bottom)** Diffusion coefficients and transmittances from two of three trials for each MS2 sample, obtained from the Litesizer 500 particle sizer (Anton Paar) are also given.

4.5 Can airborne viruses be important in ice nucleation?

Aerosols are seeds for cloud formation (Mhyre, 2013), and as stated, one of the significant uncertainties in climate change predictions (Lee et al., 2016). During the last decades of bioaerosol research on ice nucleation, it has become evident that bioaerosols and their remnants can act as efficient ice nuclei (Murray et al., 2012; Iwata et al., 2019). There are several studies which have quantified the microbial concentrations in the planetary boundary layer (Tignat-Perrier et al., 2020b, Tignat-Perrier et al., 2020a), and at higher altitudes relevant to cloud formation (Amato et al., 2019; Khaled et al., 2021, Amato et al., 2017). However, despite the known abundance of viruses compared to bacteria in ambient air, there are no studies to our knowledge which specifically investigate their role in cloud formation. Further work should be done to assess the concentrations of viruses at cloud-relevant heights.

The abundance of airborne viruses at a given time varies due to several factors, namely droplet size, evaporation rate, gravitational settling, and the viral load (Lee et al., 2016; Mittal et al., 2020). These factors make calculating airborne viral concentrations complex and subject to many limitations. Additionally, there is a multitude of environmental conditions which can affect the interaction of airborne viruses with other aerosols and their behaviour in the context of ice nucleation. These environmental factors include humidity,

radiation (particularly UVC) and temperature (Lin and Marr, 2020; Ratnesar-Shumate et al., 2020; Schuit et al., 2020). Once the virus enters the air, it is subject to all of these environmental factors and interactions with other particles. Even if the virus is not active or completely intact, this work has shown that select viruses may still retain their ice nucleation abilities. Such microphysical processes they may undergo at this stage are understudied further research is required.

Current research has shown that some airborne viruses including MS2 bacteriophage, SARS-CoV-1 and SARS-COV-2 and their remanent RNA have distinct physicochemical surfaces properties that allow them to act as effective ice nuclei at temperatures comparable to those of dust particles, which have long been considered one of the most critical global ice nuclei in the Earth's atmosphere (Murray et al., 2012; Hodinka, 2016). Like dust particles, viruses are present in massive quantities, experience transport through air, and some have been shown to effectively facilitate ice nucleation at temperatures between -13 and -17 °C. The earlier work done by Adams et al. (2021)28 suggests that they may play a more important role in the composition of marine environment INPs than those of terrestrial environments. Yet, there are many unknowns, such as their relative importance as INPs, which viruses may serve as the most effective INPs, and the microphsyicsal mechanisms by which viruses facilitate ice nucleation. Hereby, we recommend further observation, laboratory, and modelling experiments to accurately evaluate their importance.

Chapter 5

Concluding Remarks

In this study, we show for the first time that selected RNA of four different respiratory viral entities exhibit mean ice nucleation temperatures up to -13.7 °C. Adding dust-like aerosols to MS2 droplets increases ice nucleation temperatures or makes them more efficient ice nuclei. The combination of high crystallinity and polydispersity in these viruses may partially explain the effectiveness of ice nuclei. The results of this study indicate that some viruses and selected viral structures, such as RNA and proteins, might have the ability to be effective ice nuclei. Ice nucleation ability in viral structures opens new avenues for understanding water uptake in viral processes, which may have significant implications for the transmission of respiratory viruses indoors and outdoors.

As we learned from decades of bioaerosol nucleation research (Tang et al., 2022; Ariya et al., 2009; Hoose et al., 2008) airborne pathogenic particles, including some viruses and

bacteria, exhibit an extensive range of ice nucleation abilities that should be explored. As viral entities such as viral RNA and proteins are ubiquitous in natural surface waters, it is crucial to delve deeper into the impact of viruses on freezing processes in these environments. With technological advances, including in ice nucleation studies, one can better understand many other effective ice nuclei from biological origins or emerging materials from human activities. Our study emphasizes the need for continued research in this domain, with potential implications for atmospheric processes and frozen water dynamics in natural settings. Understanding the ice nucleation capabilities of viruses could provide valuable insights into climate modelling and the environmental behaviour of airborne pathogens.

Chapter 6

References

Bibliography

Adams, M. P., Atanasova, N. S., Sofieva, S., Ravantti, J., Heikkinen, A., Brasseur, Z., Duplissy, J., Bamford, D. H., & Murray, B. J. (2021). Ice nucleation by viruses and their potential for cloud glaciation. *Biogeosciences*, *18*(14), 4431–4444. https://doi.org/10.5194/bg-18-4431-2021

Amato, P., Besaury, L., Joly, M., Penaud, B., Deguillaume, L., & Delort, A.-M. (2019). Metatranscriptomic exploration of microbial functioning in clouds. *Scientific Reports*, *9*(1), 4383. https://doi.org/10.1038/s41598-019-41032-4

Amato, P., Joly, M., Besaury, L., Oudart, A., Taib, N., Moné, A. I., Deguillaume, L., Delort, A.-M., & Debroas, D. (2017). Active microorganisms thrive among extremely diverse communities in cloud water. *PLoS ONE*, *12*(8), e0182869. https://doi.org/10.1371/journal.pone.0182869

Ariya, P. A., Sun, J., Eltouny, N. A., Hudson, E. D., Hayes, C. T., & Kos, G. (2009). Physical and chemical characterization of bioaerosols – implications for nucleation processes.

International Reviews in Physical Chemistry, *28*(1), 1–32. https://doi.org/10.1080/01442350802597438

Baboomian, V. J., Gu, Y., & Nizkorodov, S. A. (2020). Photodegradation of secondary organic aerosols by long-term exposure to solar actinic radiation. *ACS Earth and Space Chemistry*, *4*(7), 1078–1089. https://doi.org/10.1021/acsearthspacechem.0c00088

Batéjat, C., Grassin, Q., Manuguerra, J.-C., & Leclercq, I. (2020, May 1). Heat inactivation of the severe acute respiratory syndrome coronavirus 2. https://doi.org/10.1101/2020.05.01.067769

Bigg, E. K. (1973). Ice nucleus concentrations in remote areas. Retrieved July 9, 2024, from https://journals.ametsoc.org/view/journals/atsc/30/6/1520-0469_1973_030_1153_incira_2_0_co_2.xml

Boldon, L., Laliberte, F., & Liu, L. (2015). Review of the fundamental theories behind small angle x-ray scattering, molecular dynamics simulations, and relevant integrated application. *Nano Reviews*, *6*, 25661. https://doi.org/10.3402/nano.v6.25661

Bose, S., Pal, D., & Ariya, P. A. (2024). On the role of starchy grains in ice nucleation processes. *ACS Food Science & Technology*, *4*(5), 1039–1051. https://doi.org/10.1021/acsfoodscitech.3c00561

Boucher, O., & Randall, D. (2013). *Climate change 2013 the physical science basis: Working group i contribution to the fifth assessment report of the intergovernmental panel on climate change*.

Breitbart, M., & Rohwer, F. (2005). Here a virus, there a virus, everywhere the same virus? *Trends in Microbiology*, *13*(6), 278–284. https://doi.org/10.1016/j.tim.2005.04.003

Burrows, S. M., McCluskey, C. S., Cornwell, G., Steinke, I., Zhang, K., Zhao, B., Zawadowicz, M., Raman, A., Kulkarni, G., China, S., Zelenyuk, A., & DeMott, P. J. (2022). Ice-nucleating particles that impact clouds and climate: Observational and modeling research needs. *Reviews of Geophysics*, *60*(2), e2021RG000745. https://doi.org/10.1029/2021RG000745

Cascajo-Castresana, M., David, R. O., Iriarte-Alonso, M. A., Bittner, A. M., & Marcolli, C. (2020). Protein aggregates nucleate ice: The example of apoferritin. *Atmospheric Chemistry and Physics*, *20*(6), 3291–3315. https://doi.org/10.5194/acp-20-3291-2020

Chen, N.-T., Cheong, N.-S., Lin, C.-Y., Tseng, C.-C., & Su, H.-J. (2021). Ambient viral and bacterial distribution during long-range transport in northern taiwan. *Environmental Pollution*, *270*, 116231. https://doi.org/10.1016/j.envpol.2020.116231

Chen, Z., Berrens, M. L., Chan, K.-T., Fan, Z., & Donadio, D. (2024). Thermodynamics of water and ice from a fast and scalable first-principles neuroevolution potential. *Journal of Chemical & Engineering Data*, *69*(1), 128–140. https://doi.org/10.1021/acs.jced.3c00561

Chou, C. (2011). *Investigation of ice nucleation properties onto soot, bioaerosol and mineral dust during different measurement campaigns* [Doctoral dissertation]. https://www.research-collection.ethz.ch/bitstream/handle/20.500.11850/43767/eth-2894-02.pdf?sequence=2&isAllowed=y

Colas de la Noue, A., Estienney, M., Aho, S., Perrier-Cornet, J.-M., de Rougemont, A., Pothier, P., Gervais, P., & Belliot, G. (2014). Absolute humidity influences the seasonal persistence and infectivity of human norovirus. *Applied and Environmental Microbiology*, *80*(23), 7196–7205. https://doi.org/10.1128/AEM.01871-14

Côté, V., Kos, G., Mortazavi, R., & Ariya, P. A. (2008). Microbial and "de novo" transformation of dicarboxylic acids by three airborne fungi. *Science of The Total Environment*, *390*(2), 530–537. https://doi.org/10.1016/j.scitotenv.2007.10.035

Davis, P., & Williams, S. (2008). Protein modification by thermal processing. *Allergy*. https://doi.org/https://doi.org/10.1111/j.1398-9995.1998.tb04975.x

DeMott, P. J. (1990). An exploratory study of ice nucleation by soot aerosols. Retrieved July 9, 2024, from https://journals.ametsoc.org/view/journals/apme/29/10/1520-0450_1990_029_1072_aesoin_2_0_co_2.xml

Dreischmeier, K., Budke, C., Wiehemeier, L., Kottke, T., & Koop, T. (2017). Boreal pollen contain ice-nucleating as well as ice-binding 'antifreeze' polysaccharides. *Scientific Reports*, *7*(1), 41890. https://doi.org/10.1038/srep41890

Du, R., Du, P., Lu, Z., Ren, W., Liang, Z., Qin, S., Li, Z., Wang, Y., & Fu, P. (2017). Evidence for a missing source of efficient ice nuclei. *Scientific Reports*, *7*(1), 39673. https://doi.org/10.1038/srep39673

Durmuş, S., & Ülgen, K. Ö. (2017). Comparative interactomics for virus–human protein–protein interactions: DNA viruses versus RNA viruses. *FEBS Open Bio*, *7*(1), 96–107. https://doi.org/10.1002/2211-5463.12167

Fahy, W. D., Maters, E. C., Miranda, R. G., Adams, M. P., Jahn, L. G., Sullivan, R. C., & Murray, B. J. (2022). Volcanic ash ice nucleation activity is variably reduced by aging in water and sulfuric acid: The effects of leaching, dissolution, and precipitation. *Environmental Science: Atmospheres*, *2*(1), 85–99. https://doi.org/10.1039/D1EA00071C

Ganguly, M., & Ariya, P. A. (2019). Ice nucleation of model nanoplastics and microplastics: A novel synthetic protocol and the influence of particle capping at diverse atmospheric environments. *ACS Earth and Space Chemistry*, *3*(9), 1729–1739. https://doi.org/10.1021/acsearthspacechem.9b00132

Ganguly, M., Dib, S., & Ariya, P. A. (2018a). Fast, cost-effective and energy efficient mercury removal-recycling technology. *Scientific Reports*, *8*(1), 16255. https://doi.org/10.1038/s41598-018-34172-6

Ganguly, M., Dib, S., & Ariya, P. A. (2018b). Purely inorganic highly efficient ice nucleating particle. *ACS Omega*, *3*(3), 3384–3395. https://doi.org/10.1021/acsomega.7b01830

Gao, K., Friebel, F., Zhou, C.-W., & Kanji, Z. A. (2022). Enhanced soot particle ice nucleation ability induced by aggregate compaction and densification. *Atmospheric Chemistry and Physics*, *22*(7), 4985–5016. https://doi.org/10.5194/acp-22-4985-2022

Geographic, N. (n.d.). *There are more viruses than stars in the universe. why do only some infect us?* Retrieved July 9, 2024, from https://www.nationalgeographic.com/science/article/factors-allow-viruses-infect-humans-coronavirus

Grassian, V. H. (2008). When size really matters: Size-dependent properties and surface chemistry of metal and metal oxide nanoparticles in gas and liquid phase environments. *The Journal of Physical Chemistry C*, *112*(47), 18303–18313. https://doi.org/10.1021/jp806073t

Gute, E., & Abbatt, J. P. D. (2020). Ice nucleating behavior of different tree pollen in the immersion mode. *Atmospheric Environment*, *231*, 117488. https://doi.org/10.1016/j.atmosenv.2020.117488

Gute, E., David, R. O., Kanji, Z. A., & Abbatt, J. P. D. (2020). Ice nucleation ability of tree pollen altered by atmospheric processing. *ACS Earth and Space Chemistry*, *4*(12), 2312–2319. https://doi.org/10.1021/acsearthspacechem.0c00218

Hartmann, S., Ling, M., Dreyer, L. S. A., Zipori, A., Finster, K., Grawe, S., Jensen, L. Z., Borck, S., Reicher, N., Drace, T., Niedermeier, D., Jones, N. C., Hoffmann, S. V., Wex, H., Rudich, Y., Boesen, T., & Šantl-Temkiv, T. (2022). Structure and protein-protein

interactions of ice nucleation proteins drive their activity. *Frontiers in Microbiology*, *13*. Retrieved December 16, 2022, from https://www.frontiersin.org/articles/10.3389/fmicb.2022.872306

Hibbs, M. (2024, July 8). Replication data for: Physicochemical properties and their impact on ice nucleation efficiency of respiratory viral RNA and proteins. https://doi.org/10.5683/SP3/ZBYBTM

Hodinka, R. L. (2016). Respiratory RNA viruses. *Microbiology Spectrum*, *4*(4), 10.1128/microbiolspec.dmih2–0028–2016. https://doi.org/10.1128/microbiolspec.dmih2-0028-2016

Hoose, C., Lohmann, U., Erdin, R., & Tegen, I. (2008). The global influence of dust mineralogical composition on heterogeneous ice nucleation in mixed-phase clouds. *Environmental Research Letters*, *3*(2), 025003. https://doi.org/10.1088/1748-9326/3/2/025003

Hoose, C., & Möhler, O. (2012). Heterogeneous ice nucleation on atmospheric aerosols: A review of results from laboratory experiments. *Atmospheric Chemistry and Physics*, *12*(20), 9817–9854. https://doi.org/10.5194/acp-12-9817-2012

Huang, S., Hu, W., Chen, J., Wu, Z., Zhang, D., & Fu, P. (2021). Overview of biological ice nucleating particles in the atmosphere. *Environment International*, *146*, 106197. https://doi.org/10.1016/j.envint.2020.106197

Iannone, R., Chernoff, D. I., Pringle, A., Martin, S. T., & Bertram, A. K. (2011). The ice nucleation ability of one of the most abundant types of fungal spores found in the atmosphere. *Atmospheric Chemistry and Physics*, *11*(3), 1191–1201. https://doi.org/10.5194/acp-11-1191-2011

Irvine, W. M., & Pollack, J. B. (1968). Infrared optical properties of water and ice spheres. *Icarus*, *8*(1), 324–360. https://doi.org/10.1016/0019-1035(68)90083-3

Iwata, A., Imura, M., Hama, M., Maki, T., Tsuchiya, N., Kunihisa, R., & Matsuki, A. (2019). Release of highly active ice nucleating biological particles associated with rain. *Atmosphere*, *10*(10), 605. https://doi.org/10.3390/atmos10100605

Kampf, G., Voss, A., & Scheithauer, S. (2020). Inactivation of coronaviruses by heat. *Journal of Hospital Infection*, *105*(2), 348–349. https://doi.org/10.1016/j.jhin.2020.03.025

Kanji, Z. A., Ladino, L. A., Wex, H., Boose, Y., Burkert-Kohn, M., Cziczo, D. J., & Krämer, M. (2017). Overview of ice nucleating particles. https://doi.org/10.1175/AMSMONOGRAPHS-D-16-0006.1

Kanji, Z. A., Welti, A., Corbin, J. C., & Mensah, A. A. (2020). Black carbon particles do not matter for immersion mode ice nucleation. *Geophysical Research Letters*, *47*(11), e2019GL086764. https://doi.org/10.1029/2019GL086764

Kaufmann, L., Marcolli, C., Hofer, J., Pinti, V., Hoyle, C. R., & Peter, T. (2016). Ice nucleation efficiency of natural dust samples in the immersion mode. *Atmospheric*

Chemistry and Physics, *16*(17), 11177–11206. https://doi.org/10.5194/acp-16-11177-2016

Kaur, J., Ganguly, M., Rangel-Alvardo, R., Pal, D., Hall, R., & Ariya, P. A. (2022). Ice nucleation of pharmaceutical and synthetic organic emerging contaminants: The impact of selected environmental conditions. *ACS Earth and Space Chemistry*, *6*(9), 2236–2249. https://doi.org/10.1021/acsearthspacechem.2c00187

Khaled, A., Zhang, M., Amato, P., Delort, A.-M., & Ervens, B. (2021). Biodegradation by bacteria in clouds: An underestimated sink for some organics in the atmospheric multiphase system. *Atmospheric Chemistry and Physics*, *21*(4), 3123–3141. https://doi.org/10.5194/acp-21-3123-2021

Kim, K.-H., Kabir, E., & Jahan, S. A. (2018). Airborne bioaerosols and their impact on human health. *Journal of Environmental Sciences*, *67*, 23–35. https://doi.org/10.1016/j.jes.2017.08.027

Koohbor, B., Ruzskowski, J., Myren, K., Dinse, J., Smith, A., & Bering, E. (2023). The effects of temperature and humidity on aerosol optical properties. *2023 Regional Student Conferences*. https://doi.org/10.2514/6.2023-72180

Kunert, A. T., Pöhlker, M. L., Tang, K., Krevert, C. S., Wieder, C., Speth, K. R., Hanson, L. E., Morris, C. E., Schmale III, D. G., Pöschl, U., & Fröhlich-Nowoisky, J. (2019). Macromolecular fungal ice nuclei in *Fusarium*: Effects

of physical and chemical processing. *Biogeosciences*, *16*(23), 4647–4659. https://doi.org/10.5194/bg-16-4647-2019

Laaksonen, A., & Malila, J. (2022, January 1). Chapter 10 - ice nucleation. In A. Laaksonen & J. Malila (Eds.), *Nucleation of water* (pp. 209–248). Elsevier. https://doi.org/10.1016/B978-0-12-814321-6.00018-X

Lee, L. A., Reddington, C. L., & Carslaw, K. S. (2016). On the relationship between aerosol model uncertainty and radiative forcing uncertainty. *Proceedings of the National Academy of Sciences*, *113*(21), 5820–5827. https://doi.org/10.1073/pnas.1507050113

Lelieveld, J., Pozzer, A., Pöschl, U., Fnais, M., Haines, A., & Münzel, T. (2020). Loss of life expectancy from air pollution compared to other risk factors: A worldwide perspective. *Cardiovascular Research*, *116*(11), 1910–1917. https://doi.org/10.1093/cvr/cvaa025

Li, T., Senesi, A. J., & Lee, B. (2016). Small angle x-ray scattering for nanoparticle research. *Chemical Reviews*, *116*(18), 11128–11180. https://doi.org/10.1021/acs.chemrev.5b00690

Lin, K., & Marr, L. C. (2020). Humidity-dependent decay of viruses, but not bacteria, in aerosols and droplets follows disinfection kinetics. *Environmental Science & Technology*, *54*(2), 1024–1032. https://doi.org/10.1021/acs.est.9b04959

Lukas, M., Schwidetzky, R., Kunert, A. T., Pöschl, U., Fröhlich-Nowoisky, J., Bonn, M., & Meister, K. (2020). Electrostatic interactions control the functionality of bacterial

ice nucleators. *Journal of the American Chemical Society*, *142*(15), 6842–6846. https://doi.org/10.1021/jacs.9b13069

Lukas, M., Schwidetzky, R., Eufemio, R. J., Bonn, M., & Meister, K. (2022). Toward understanding bacterial ice nucleation. *The Journal of Physical Chemistry B*, *126*(9), 1861–1867. https://doi.org/10.1021/acs.jpcb.1c09342

Marcolli, C., Mahrt, F., & Kärcher, B. (2021). Soot PCF: Pore condensation and freezing framework for soot aggregates. *Atmospheric Chemistry and Physics*, *21*(10), 7791–7843. https://doi.org/10.5194/acp-21-7791-2021

Maters, E. C., Dingwell, D. B., Cimarelli, C., Müller, D., Whale, T. F., & Murray, B. J. (2019). The importance of crystalline phases in ice nucleation by volcanic ash. *Atmospheric Chemistry and Physics*, *19*(8), 5451–5465. https://doi.org/10.5194/acp-19-5451-2019

Matus, A. V., & L'Ecuyer, T. S. (2017). The role of cloud phase in earth's radiation budget. *Journal of Geophysical Research: Atmospheres*, *122*(5), 2559–2578. https://doi.org/10.1002/2016JD025951

Mhyre, G. (2013). Aerosols and their relation to global climate and climate sensitivity. *Nature Education Knowledge*, *4*(5), 7.

Mittal, R., Meneveau, C., & Wu, W. ((2020). A mathematical framework for estimating risk of airborne transmission of COVID-19 with application to face mask use and social distancing. *Physics of Fluids*, *32*(10), 101903. https://doi.org/10.1063/5.0025476

Moelling, K., & Broecker, F. (2019). Viruses and evolution – viruses first? a personal perspective. *Frontiers in Microbiology*, *10*. https://doi.org/10.3389/fmicb.2019.00523

Morawska, L., Buonanno, G., Mikszewski, A., & Stabile, L. (2022). The physics of respiratory particle generation, fate in the air, and inhalation. *Nature Reviews Physics*, *4*(11), 723–734. https://doi.org/10.1038/s42254-022-00506-7

Mortazavi, R., Hayes, C. T., & Ariya, P. A. (2008). Ice nucleation activity of bacteria isolated from snow compared with organic and inorganic substrates. *Environmental Chemistry*, *5*(6), 373. https://doi.org/10.1071/EN08055

Murray, B. J., O'Sullivan, D., Atkinson, J. D., & Webb, M. E. (2012). Ice nucleation by particles immersed in supercooled cloud droplets. *Chemical Society Reviews*, *41*(19), 6519. https://doi.org/10.1039/c2cs35200a

Pal, D. (2023). *New insights in aerosol science using optical and digital holographic microscopy: From nano-aerosols to cloud droplets* [Doctoral dissertation].

Pal, D., Amyot, M., Liang, C., & Ariya, P. A. (2023). Real-time 4d tracking of airborne virus-laden droplets and aerosols. *Communications Engineering*, *2*(1), 1–15. https://doi.org/10.1038/s44172-023-00088-x

Pastorino, B., Touret, F., Gilles, M., de Lamballerie, X., & Charrel, R. N. (2020). Heat inactivation of different types of SARS-CoV-2 samples: What protocols for biosafety,

molecular detection and serological diagnostics? *Viruses*, *12*(7), 735. https://doi.org/10.3390/v12070735

Penner, J. E., Andreae, M., Annegarn, H., Barrie, L., Feichter, J., Hegg, D., Jayaraman, A., Leaitch, R., Murphy, D., Nganga, J., Pitari, G., Ackerman, A., Adams, P., Austin, P., Boers, R., Boucher, O., Chin, M., Chuang, C., Collins, B., ... Prospero, J. (2018). *Aerosols, their direct and indirect effects* (tech. rep.). Intergovernmental Panel on Climate Change.

Pouleur, S., Richard, C., Martin, J. G., & Antoun, H. (1992). Ice nucleation activity in fusarium acuminatum and fusarium avenaceum. *Applied and Environmental Microbiology*, *58*(9), 2960–2964. https://doi.org/10.1128/aem.58.9.2960-2964.1992

Pruppacher, H. R., & Klett, J. D. (1997). *Microphysics of clouds and precipitation* (Second). Springer.

Pummer, B. G., Bauer, H., Bernardi, J., Bleicher, S., & Grothe, H. (2012). Suspendable macromolecules are responsible for ice nucleation activity of birch and conifer pollen. *Atmospheric Chemistry and Physics*, *12*(5), 2541–2550. https://doi.org/10.5194/acp-12-2541-2012

Raatikainen, T., Prank, M., Ahola, J., Kokkola, H., Tonttila, J., & Romakkaniemi, S. (2022). The effect of marine ice-nucleating particles on mixed-phase clouds. *Atmospheric Chemistry and Physics*, *22*(6), 3763–3778. https://doi.org/10.5194/acp-22-3763-2022

Rangel-Alvarado, R., Pal, D., & Ariya, P. (2021, October 13). PM $_{2.5}$ decadal data in cold vs. mid-climate airports: COVID-19 era and a call for sustainable air quality policy. https://doi.org/10.2139/ssrn.3941685

Ratnesar-Shumate, S., Williams, G., Green, B., Krause, M., Holland, B., Wood, S., Bohannon, J., Boydston, J., Freeburger, D., Hooper, I., Beck, K., Yeager, J., Altamura, L. A., Biryukov, J., Yolitz, J., Schuit, M., Wahl, V., Hevey, M., & Dabisch, P. (2020). Simulated sunlight rapidly inactivates SARS-CoV-2 on surfaces. *The Journal of Infectious Diseases*, *222*(2), 214–222. https://doi.org/10.1093/infdis/jiaa274

Rogers, R. R., & Yau, M. K. (1989). *A short course in cloud physics* (Third). Elsevier.

SasView. (n.d.). *SasView*. Retrieved July 9, 2024, from https://sasview.github.io/

SasView user documentation — SasView 5.0.6 documentation. (n.d.). Retrieved July 9, 2024, from https://www.sasview.org/docs/user/user.html

Schaller. (2019, September 24). *1.3: Activation barriers* [Chemistry LibreTexts]. Retrieved July 10, 2024, from https://chem.libretexts.org/Bookshelves/General_Chemistry/Book%3A_Structure_and_Reactivity_in_Organic_Biological_and_Inorganic_Chemistry_(Schaller) /IV % 3A__Reactivity_in_Organic_Biological_and_Inorganic_Chemistry_2 / 01 % 3A_Reaction_Kinetics/1.03%3A_Activation_Barriers

Schuit, M., Ratnesar-Shumate, S., Yolitz, J., Williams, G., Weaver, W., Green, B., Miller, D., Krause, M., Beck, K., Wood, S., Holland, B., Bohannon, J., Freeburger, D., Hooper, I., Biryukov, J., Altamura, L. A., Wahl, V., Hevey, M., & Dabisch, P. (2020). Airborne SARS-CoV-2 is rapidly inactivated by simulated sunlight. *The Journal of Infectious Diseases*, *222*(4), 564–571. https://doi.org/10.1093/infdis/jiaa334

Seifert, P., Ansmann, A., Groß, S., Freudenthaler, V., Heinold, B., Hiebsch, A., Mattis, I., Schmidt, J., Schnell, F., Tesche, M., Wandinger, U., & Wiegner, M. (2011). Ice formation in ash-influenced clouds after the eruption of the eyjafjallajökull volcano in april 2010. *Journal of Geophysical Research: Atmospheres*, *116*. https://doi.org/10.1029/2011JD015702

Sun, J., & Ariya, P. A. (2006). Atmospheric organic and bio-aerosols as cloud condensation nuclei (CCN): A review. *Atmospheric Environment*, *40*(5), 795–820. https://doi.org/10.1016/j.atmosenv.2005.05.052

Tan, I. (2022). *Formation & growth of ice crystals*. https://mycourses2.mcgill.ca/d2l/le/lessons/556905/topics/6349222

Tang, K., Sánchez-Parra, B., Yordanova, P., Wehking, J., Backes, A. T., Pickersgill, D. A., Maier, S., Sciare, J., Pöschl, U., Weber, B., & Fröhlich-Nowoisky, J. (2022). Bioaerosols and atmospheric ice nuclei in a mediterranean dryland: Community changes related to rainfall. *Biogeosciences*, *19*(1), 71–91. https://doi.org/10.5194/bg-19-71-2022

Tignat-Perrier, R., Dommergue, A., Thollot, A., Magand, O., Vogel, T. M., & Larose, C. (2020a). Microbial functional signature in the atmospheric boundary layer. *Biogeosciences*, *17*(23), 6081–6095. https://doi.org/10.5194/bg-17-6081-2020

Tignat-Perrier, R., Dommergue, A., Vogel, T. M., & Larose, C. (2020b). Microbial ecology of the planetary boundary layer. *Atmosphere*, *11*(12), 1296. https://doi.org/10.3390/atmos11121296

Tobo, Y. (2016). An improved approach for measuring immersion freezing in large droplets over a wide temperature range. *Scientific Reports*, *6*(1), 32930. https://doi.org/10.1038/srep32930

Turgeon, N., Toulouse, M.-J., Martel, B., Moineau, S., & Duchaine, C. (2014). Comparison of five bacteriophages as models for viral aerosol studies. *Applied and Environmental Microbiology*, *80*(14), 4242–4250. https://doi.org/10.1128/AEM.00767-14

Vali, G. (1971). Quantitative evaluation of experimental results an the heterogeneous freezing nucleation of supercooled liquids. *Journal of the Atmospheric Sciences*, *28*(3), 402–409. https://doi.org/10.1175/1520-0469(1971)028⟨0402:QEOERA⟩2.0.CO;2

Wagner, R., Ickes, L., Bertram, A. K., Els, N., Gorokhova, E., Möhler, O., Murray, B. J., Umo, N. S., & Salter, M. E. (2021). Heterogeneous ice nucleation ability of aerosol particles generated from arctic sea surface microlayer and surface seawater samples

at cirrus temperatures. *Atmospheric Chemistry and Physics*, *21*(18), 13903–13930. https://doi.org/10.5194/acp-21-13903-2021

Wagner, R., Kiselev, A., Möhler, O., Saathoff, H., & Steinke, I. (2016). Pre-activation of ice-nucleating particles by the pore condensation and freezing mechanism. *Atmospheric Chemistry and Physics*, *16*(4), 2025–2042. https://doi.org/10.5194/acp-16-2025-2016

Walhout, E. Q., Yu, H., Thrasher, C., Shusterman, J. M., & O'Brien, R. E. (2019). Effects of photolysis on the chemical and optical properties of secondary organic material over extended time scales. *ACS Earth and Space Chemistry*, *3*(7), 1226–1236. https://doi.org/10.1021/acsearthspacechem.9b00109

Whale, T. F. (2018, January 1). Chapter 2 - ice nucleation in mixed-phase clouds. In C. Andronache (Ed.), *Mixed-phase clouds* (pp. 13–41). Elsevier. https://doi.org/10.1016/B978-0-12-810549-8.00002-7

Wilson, T. W., Ladino, L. A., Alpert, P. A., Breckels, M. N., Brooks, I. M., Browse, J., Burrows, S. M., Carslaw, K. S., Huffman, J. A., Judd, C., Kilthau, W. P., Mason, R. H., McFiggans, G., Miller, L. A., Nájera, J. J., Polishchuk, E., Rae, S., Schiller, C. L., Si, M., ... Murray, B. J. (2015). A marine biogenic source of atmospheric ice-nucleating particles. *Nature*, *525*(7568), 234–238. https://doi.org/10.1038/nature14986

Wolber, P. K. (1993, January 1). Bacterial ice nucleation. In A. H. Rose (Ed.), *Advances in microbial physiology* (pp. 203–237, Vol. 34). Academic Press. https://doi.org/10.1016/S0065-2911(08)60030-2

Yang, W., & Marr, L. C. (2012). Mechanisms by which ambient humidity may affect viruses in aerosols. *Applied and Environmental Microbiology*, *78*(19), 6781–6788. https://doi.org/10.1128/AEM.01658-12

Zelinka, M. D., Randall, D. A., Webb, M. J., & Klein, S. A. (2017). Clearing clouds of uncertainty. *Nature Climate Change*, *7*(10), 674–678. https://doi.org/10.1038/nclimate3402

Appendix A

Supplementary Information

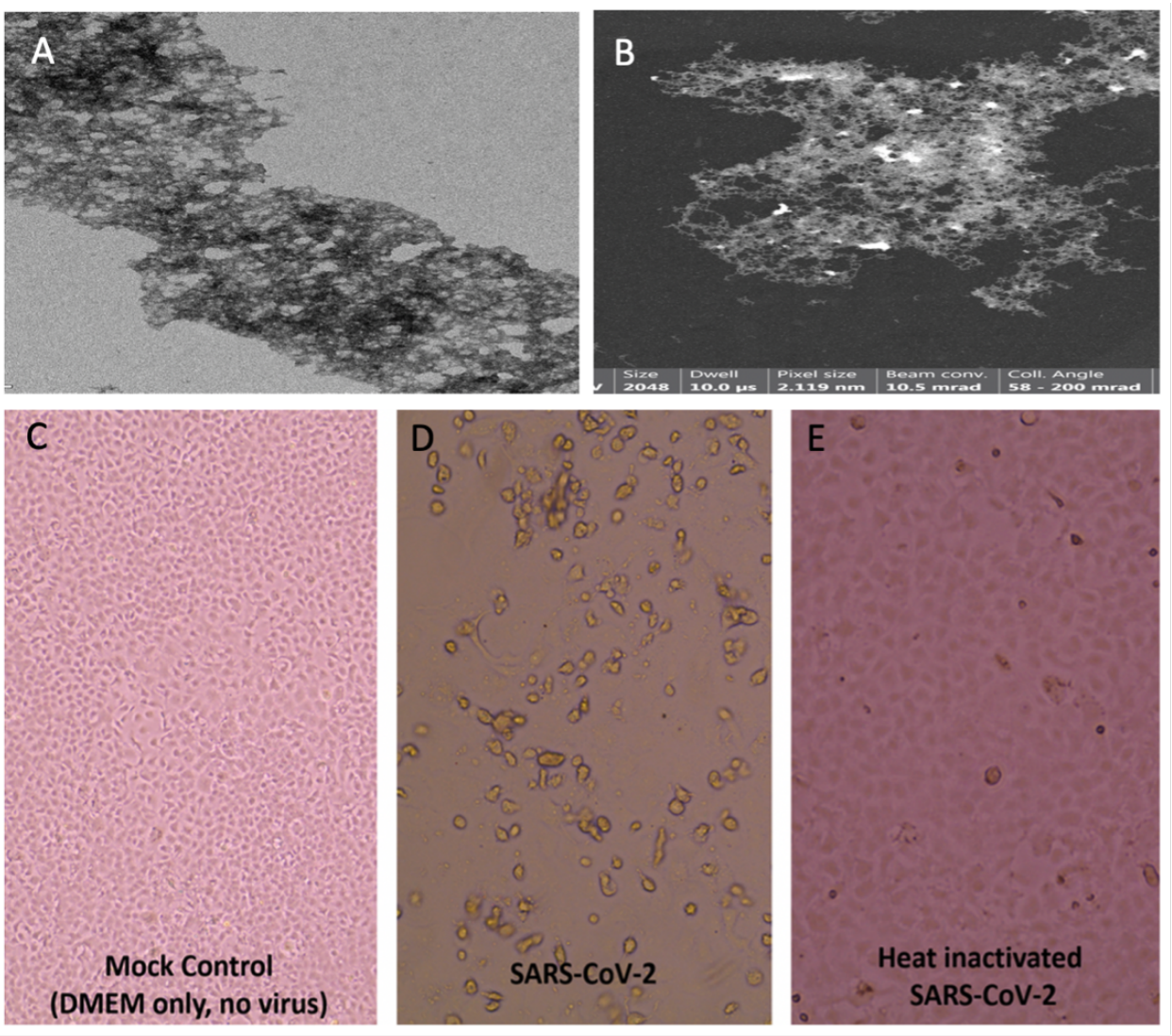

Figure A.1: A, B) Selected S/TEM images of drops of diluted Bacteriophage MS2 samples analyzed to find the MS2 particles in aggregates. Imaged using Spirit 120 kV TEM and Talos F200X 200 kV TEM respectively. Optical microscopy Images C) Cytopathic effect in Vero E6 cells after inoculation with Mock. D) SARS-CoV-2 virus. E) Heat inactivated SARS-CoV-2, no CPE detected after 7 days indicates no remaining viral activity and samples can then be removed from the BSL3

Descriptions | Graphic Summary | Alignments | Taxonomy

Sequences producing significant alignments Download | New Select columns | Show 100

select all *100 sequences selected* GenBank | Graphics | Distance tree of results | New MSA Viewer

Description	Scientific Name	Max Score	Total Score	Query Cover	E value	Per. Ident	Acc. Len	Accession
Severe acute respiratory syndrome coronavirus 2 isolate hCoV-19/Switzerland/VD-CHUV-GEN2511/2020 geno...	Severe acute res...	54983	54983	99%	0.0	99.99%	29903	OU267426.1
Severe acute respiratory syndrome coronavirus 2 isolate hCoV-19/Switzerland/VD-CHUV-GEN2967/2020 geno...	Severe acute res...	54983	54983	99%	0.0	99.99%	29903	OU267425.1
Severe acute respiratory syndrome coronavirus 2 isolate hCoV-19/Switzerland/VD-CHUV-GEN2958/2020 geno...	Severe acute res...	54983	54983	99%	0.0	99.99%	29903	OU267423.1
Severe acute respiratory syndrome coronavirus 2 isolate hCoV-19/Switzerland/VD-CHUV-GEN2978/2020 geno...	Severe acute res...	54983	54983	99%	0.0	99.99%	29903	OU267420.1
Severe acute respiratory syndrome coronavirus 2 isolate hCoV-19/Switzerland/VD-CHUV-GEN2528/2020 geno...	Severe acute res...	54983	54983	99%	0.0	99.99%	29903	OU267419.1
Severe acute respiratory syndrome coronavirus 2 isolate hCoV-19/Switzerland/VD-CHUV-GEN2472/2020 geno...	Severe acute res...	54983	54983	99%	0.0	99.99%	29903	OU267417.1
Severe acute respiratory syndrome coronavirus 2 isolate hCoV-19/Switzerland/VD-CHUV-GEN2484/2020 geno...	Severe acute res...	54983	54983	99%	0.0	99.99%	29903	OU267415.1
Severe acute respiratory syndrome coronavirus 2 isolate hCoV-19/Switzerland/VD-CHUV-GEN2512/2020 geno...	Severe acute res...	54983	54983	99%	0.0	99.99%	29903	OU267414.1
Severe acute respiratory syndrome coronavirus 2 isolate hCoV-19/Switzerland/VD-CHUV-GEN2478/2020 geno...	Severe acute res...	54983	54983	99%	0.0	99.99%	29903	OU267413.1
Severe acute respiratory syndrome coronavirus 2 isolate hCoV-19/Switzerland/VD-CHUV-GEN2488/2020 geno...	Severe acute res...	54983	54983	99%	0.0	99.99%	29903	OU267412.1
Severe acute respiratory syndrome coronavirus 2 isolate hCoV-19/Switzerland/VD-CHUV-GEN2479/2020 geno...	Severe acute res...	54983	54983	99%	0.0	99.99%	29903	OU267411.1
Severe acute respiratory syndrome coronavirus 2 isolate hCoV-19/Switzerland/VD-CHUV-GEN2521/2020 geno...	Severe acute res...	54983	54983	99%	0.0	99.99%	29903	OU267410.1
Severe acute respiratory syndrome coronavirus 2 isolate hCoV-19/Switzerland/VD-CHUV-GEN2517/2020 geno...	Severe acute res...	54983	54983	99%	0.0	99.99%	29903	OU267409.1
Severe acute respiratory syndrome coronavirus 2 isolate hCoV-19/Switzerland/VD-CHUV-GEN2476/2020 geno...	Severe acute res...	54983	54983	99%	0.0	99.99%	29903	OU267408.1
Severe acute respiratory syndrome coronavirus 2 isolate hCoV-19/Switzerland/VD-CHUV-GEN2487/2020 geno...	Severe acute res...	54983	54983	99%	0.0	99.99%	29903	OU267403.1
Severe acute respiratory syndrome coronavirus 2 isolate hCoV-19/Switzerland/VD-CHUV-GEN2471/2020 geno...	Severe acute res...	54983	54983	99%	0.0	99.99%	29903	OU267398.1
Severe acute respiratory syndrome coronavirus 2 genome assembly, complete genome: monopartite	Severe acute res...	54983	54983	99%	0.0	99.99%	29903	OA967097.1
Severe acute respiratory syndrome coronavirus 2 genome assembly, complete genome: monopartite	Severe acute res...	54983	54983	99%	0.0	99.99%	29903	OA964362.1
Severe acute respiratory syndrome coronavirus 2 genome assembly, complete genome: monopartite	Severe acute res...	54983	54983	99%	0.0	99.99%	29903	OA964256.1
Severe acute respiratory syndrome coronavirus 2 isolate Switzerland/GE-SNRCI-8301/2020 genome assembly,...	Severe acute res...	54983	54983	99%	0.0	99.99%	29836	FR993513.1
Severe acute respiratory syndrome coronavirus 2 isolate Switzerland/GE-SNRCI-9136/2020 genome assembly,...	Severe acute res...	54983	54983	99%	0.0	99.99%	29834	FR993438.1

Figure A.2: BLASTN, using the betacornavirus genomic database, result of the sequence genome of the SARS-CoV-2 sample. GenBank ID for the sequence is MN908947.3.

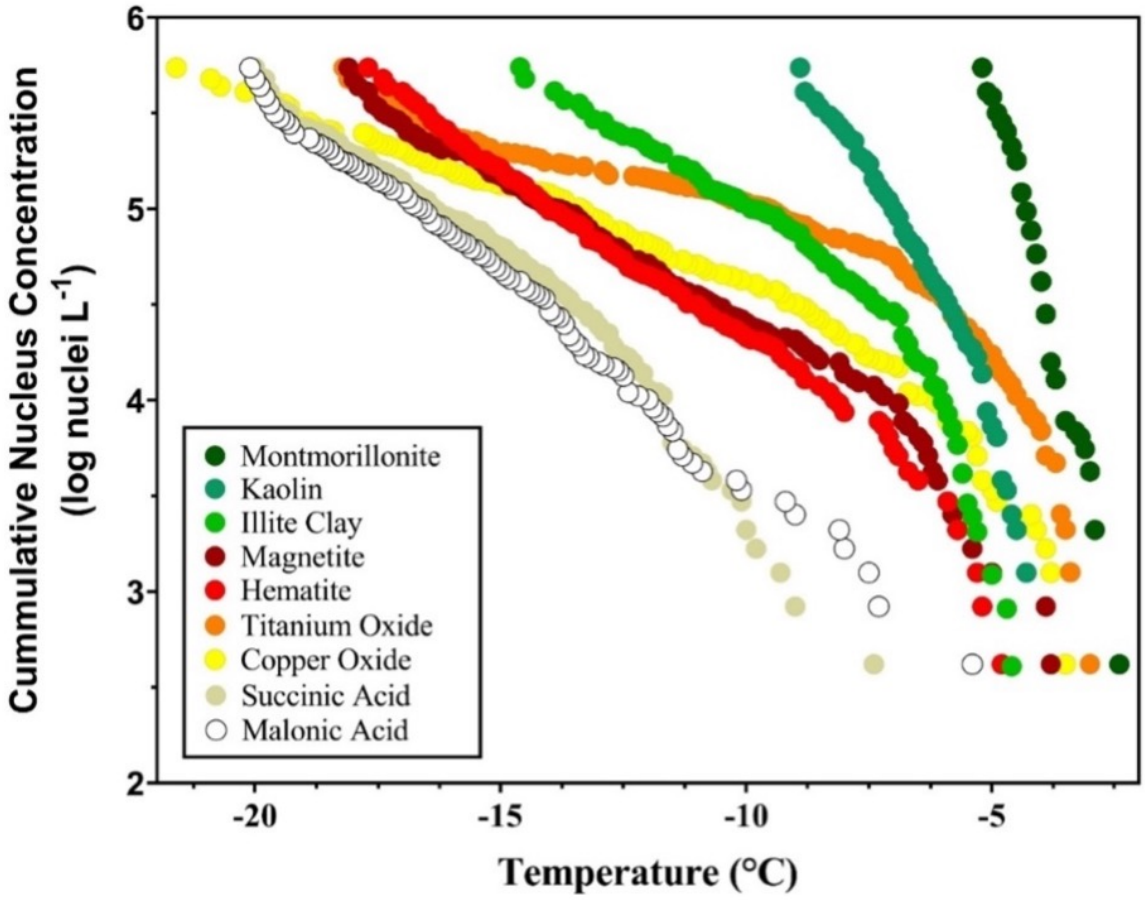

Figure A.3: Cumulative ice nucleus concentrations for selected airborne contaminants.

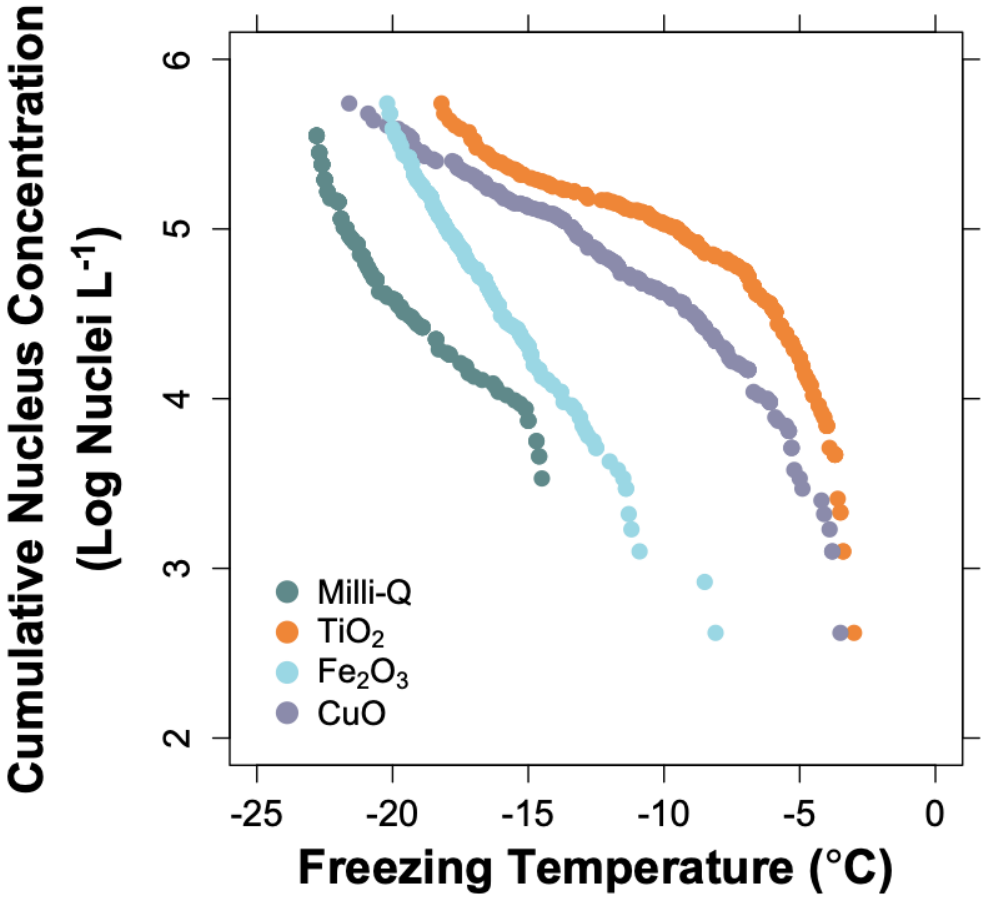

Figure A.4: Cumulative ice nucleus concentrations for TiO_2, Fe_2O_3, and CuO compared to the Milli-Q reference.

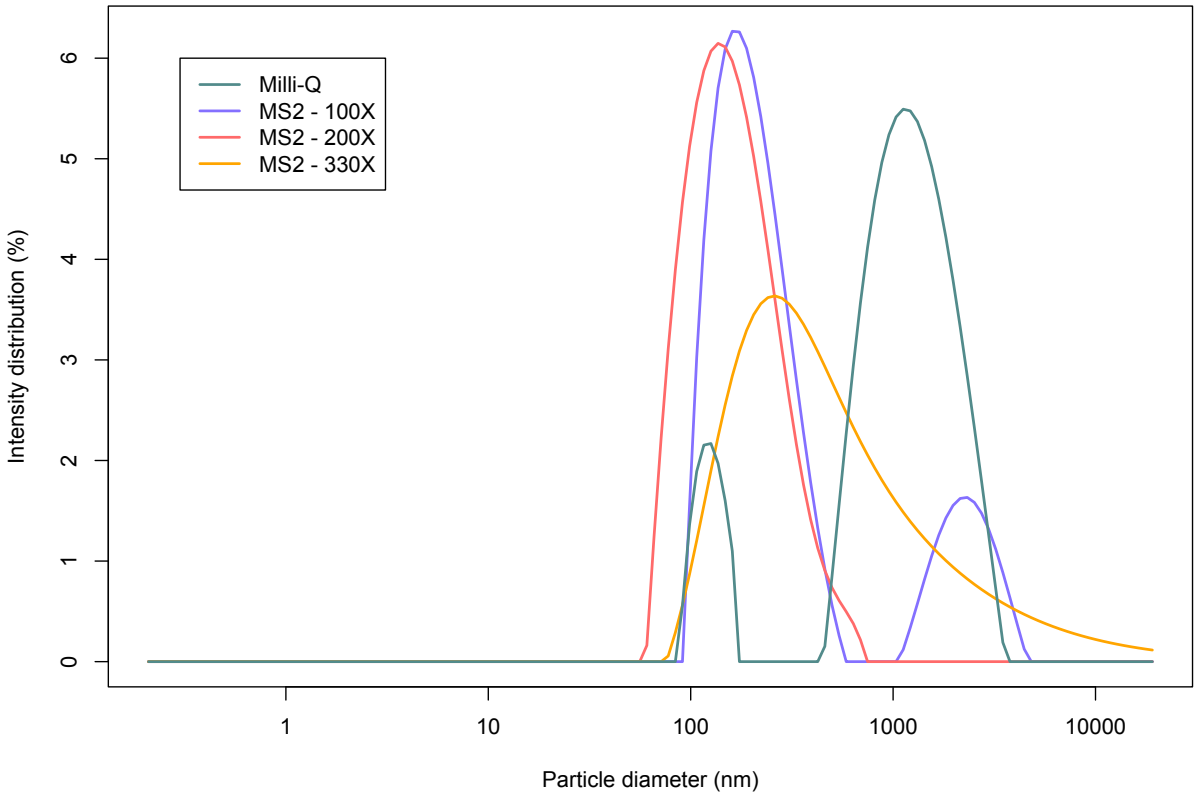

Figure A.5: Intensity-weighted size distribution vs. particle diameters for MS2 samples at various dilution factors. Data was obtained from the Litesizer particle sizer 500 (Anton Paar).

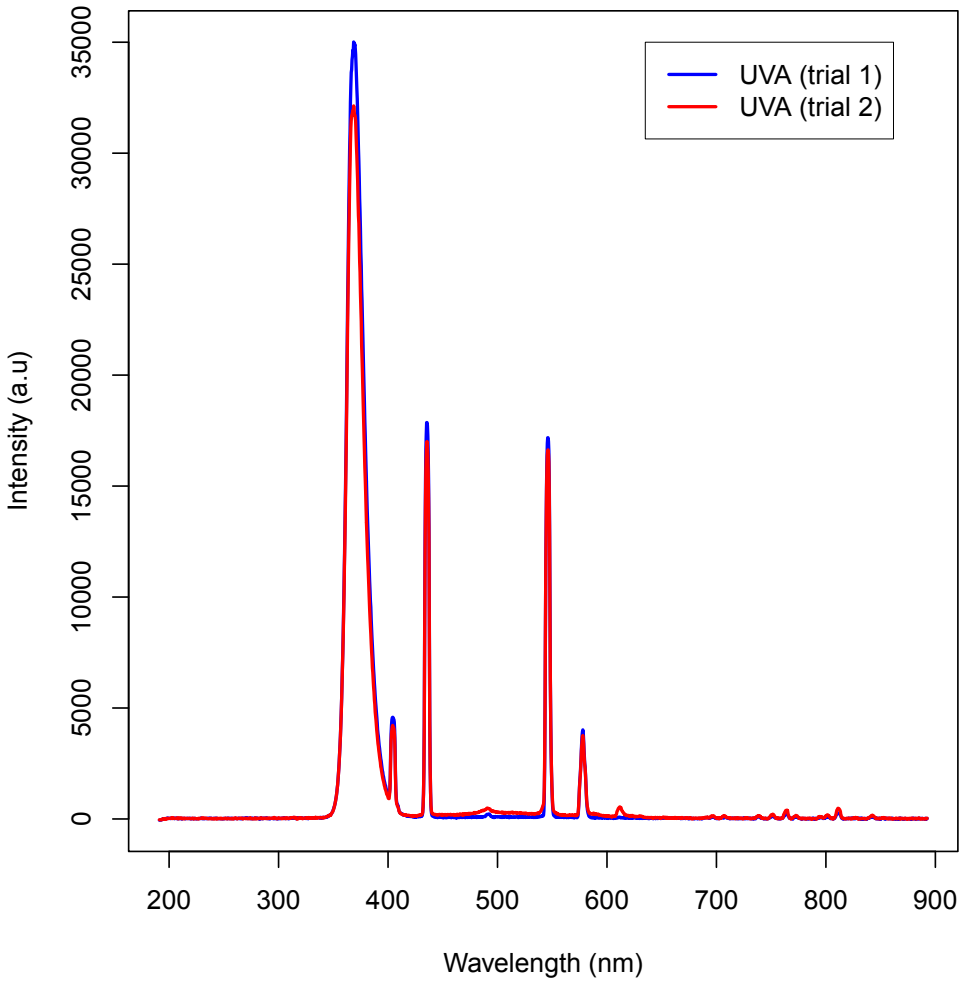

.

Figure A.6: Intensity vs. wavelength of the UVA lamp used in experiments (2 trials).